


# Lobular homology in cerebellar hemispheres of humans, non-human primates and rodents: a structural, axonal tracing and molecular expression analysis

Yuanjun Luo<sup>1</sup> · Hirofumi Fujita<sup>1,4</sup> · Hermina Nedelescu<sup>1</sup> · Mohammad Shahangir Biswas<sup>1</sup> · Chika Sato<sup>6</sup> · Sarah Ying<sup>1,5</sup> · Mayu Takahashi<sup>1</sup> · Keiichi Akita<sup>2</sup> · Tatsuya Higashi<sup>6</sup> · Ichio Aoki<sup>6</sup> · Izumi Sugihara<sup>1,3</sup> 

Received: 13 February 2016 / Accepted: 28 April 2017 / Published online: 15 May 2017  
© Springer-Verlag Berlin Heidelberg 2017

**Abstract** Comparative neuroanatomy provides insights into the evolutionary functional adaptation of specific mammalian cerebellar lobules, in which the lobulation pattern and functional localization are conserved. However, accurate identification of homologous lobules among mammalian species is challenging. In this review, we discuss the inter-species homology of crus I and II lobules which occupy a large volume in the posterior cerebellar hemisphere, particularly in humans. Both crus I/II in humans are homologous to crus I/II in non-human primates, according to Paxinos and colleagues; however, this area has been defined as crus I alone in non-human primates, according to Larsell and Brodal. Our

neuroanatomical analyses in humans, macaques, marmosets, rats, and mice demonstrate that both crus I/II in humans are homologous to crus I/II or crus I alone in non-human primates, depending on previous definitions, and to crus I alone in rodents. Here, we refer to the region homologous to human crus I/II lobules as “ansiform area (AA)” across animals. Our results show that the AA’s olivocerebellar climbing fiber and Purkinje cell projections as well as aldolase C gene expression patterns are both distinct and conserved in marmosets and rodents. The relative size of the AA, as represented by the AA volume fraction in the whole cerebellum was 0.34 in human, 0.19 in macaque, and approximately 0.1 in marmoset and rodents. These results indicate that the AA reflects an evolutionarily conserved structure in the mammalian cerebellum, which is characterized by distinct connectivity from neighboring lobules and a massive expansion in skillful primates.

Yuanjun Luo and Hirofumi Fujita contributed equally to this work.

✉ Izumi Sugihara  
isugihara.phy1@tmd.ac.jp

- <sup>1</sup> Department of Systems Neurophysiology, Tokyo Medical and Dental University Graduate School, 1-5-45 Yushima, Bunkyo-ku, Tokyo 113-8519, Japan
- <sup>2</sup> Department of Clinical Anatomy, Tokyo Medical and Dental University, 1-5-45 Yushima, Bunkyo-ku, Tokyo 113-8519, Japan
- <sup>3</sup> Center for Brain Integration Research, Tokyo Medical and Dental University, 1-5-45 Yushima, Bunkyo-ku, Tokyo 113-8519, Japan
- <sup>4</sup> Department of Otolaryngology-Head and Neck Surgery, Johns Hopkins University School of Medicine, 720 Rutland Ave., Baltimore, MD 21205, USA
- <sup>5</sup> Departments of Radiology, Neurology, and Ophthalmology, Johns Hopkins University School of Medicine, 600 N. Wolfe St., Baltimore, MD 21287, USA
- <sup>6</sup> Department of Molecular Imaging and Theranostics, National Institute of Radiological Sciences (NIRS), QST, 4-9-1 Anagawa, Inage-ku, Chiba 263-8555, Japan

**Keywords** Crus I · Semilunar lobule · Ansiform lobule · Cerebellum · Marmoset · Magnetic resonance imaging

## Introduction

The foliation of the mammalian cerebellum into multiple lobules is one of the basic landmarks related to cerebellar functional localization: the presence of location-based neuronal activity with specific physiological characteristics (MacKay and Murphy 1979; Brodal 1981; Voogd 2004; Glickstein et al. 2011). In the vermis, the lobular organization of the cerebellum is conserved among various mammals (Lobules I–X of Larsell 1970). Although species-dependent differences in lobular structure are greater in the hemisphere compared to those in the vermis, the

basic lobular organization in the hemisphere is regarded as commonly shared by all mammals (Bolk 1906; Larsell 1970). The current definition of cerebellar lobules is owed primarily to comparative morphological studies by Larsell (1970), as well as Larsell and Jansen (1972), who examined the foliation of the cerebellar surface and in mid-sagittal sections. Subsequent publications that showed cerebellar lobules in series of sections adopted Larsell's definition (human: Schmahmann et al. 1999; macaque: Madigan and Carpenter 1971; Paxinos et al. 2009; marmoset: Fujita et al. 2010; Paxinos et al. 2011; rat: Voogd 2004; Paxinos and Watson 2007; Swanson 1998; mouse: Marani and Voogd 1979; Paxinos and Franklin 2001; Fujita et al. 2014).

Among the ten lobules in the mammalian cerebellum, lobules VI and VII are well-developed in the hemisphere. More specifically, the hemispheric extension from the rostral part of lobule VII expands remarkably in the lateral hemisphere forming two major lobules; crus I and crus II of the ansiform lobule (Bolk 1906). Crus I and crus II are the most prominent regions in the human cerebellum, occupying a substantially large volume of the posterior lateral hemisphere relative to other species (Balsters et al. 2010). Due to this enlargement, accurate identification of the homologous lobules in this area requires a multi-level experimental approach to highlight the topographical details shared across species. In fact, there exists an inconsistency in the previously defined crus I and crus II, as well as, adjacent lobules within the primate literature (Larsell 1970; Madigan and Carpenter 1971; Brodal 1979; Paxinos et al. 2000; Kelly and Strick 2003; Glickstein et al. 2011; Fujita et al. 2010; Paxinos et al. 2011), and between primates and rodents (Paxinos and Watson 2007; Voogd 2004; Paxinos and Franklin 2001; Fujita et al. 2014). Therefore, we examined in detail the surface, section morphology, axonal projection, and molecular expression pattern of crus I and II across five species of the Euarchontoglires clade (human, macaque, marmoset, rat and mouse; Springer et al. 2004). We then compared key morphological features among species in our preparation to those in previous publications to demonstrate the appropriate identification of homologous lobules in the crus I/II area.

The importance of correctly identifying the crus I/II area lies in its functional significance. Human imaging studies of the cerebellum suggest that crus I/II is primarily involved in cognitive, executive, language processing, and saccadic functions (Stoodley and Schmahmann 2009; Batson et al. 2015; D'Mello and Stoodley 2015). Non-human primate studies characterize crus I/II by their connectivity to the prefrontal cortex underlying non-motor functions (Strick et al. 2009). Conversely, crus I/II or crus II alone is known as the lobule which is responsive to somatosensory stimulation of vibrissae, perioral area, and motor activity of mouth and tongue in rodents (Shambes

et al. 1978; Welsh et al. 1995). Although the functional difference in this area may be due to species differences, an alternate possibility is that lobule nomenclature in the hemisphere is inconsistent between rodents and primates. Therefore, we review in detail (1) axonal projections, which underlie the functional connectivity between regions, (2) molecular expression patterns, and (3) volume fractions of crus I/II and neighboring areas to discuss the functional significance of this region.

## Materials and methods

All procedures performed in studies involving animals were in accordance with the ethical standards of the institution at which the studies were conducted. The experimental protocols were approved by the Institutional Animal Care and Use Committee of Tokyo Medical and Dental University (Rat and mouse: No. 0060121, 0070133, 0080110; Marmoset: 0080111, 0090155). Cadavers were donated to the Department of Anatomy, Tokyo Medical and Dental University, Japan. Each donor provided written consent agreeing to donate his/her body for clinical anatomy studies. The consenting document met the expectation of Japanese law "Act on Body Donation for Medical and Dental Education". The use of human samples was approved by the Ethics Committee of Tokyo Medical and Dental University (No. M2016-095) and National Institute of Radiological Sciences (No. 16-022).

## Subjects

### *Humans*

Three human cerebellums were dissected and kept soaked in 10% formalin for 2–24 months. Subsequently, the arachnoid and vasculature were removed from the cerebellar surface. To visualize lobular arrangement, photographs of the surface of the cerebellar hemispheres were taken with a digital camera (FinePIX602, Fuji film, Tokyo, Japan) with a ring-shaped flash illumination around the lens to minimize shadow and light reflection. Three-dimensional (3D) T1-weighted magnetic resonance (MR) images were obtained with an inversion recovery-prepared fast spoiled gradient echo (BRAVO, GE) sequence using a GE 3 Tesla scanner with the following parameters: repetition time (TR) = 6.8 ms, effective echo time (TE) = 3.0 ms, inversion time (TI) = 400 ms, flip angle = 20°, matrix size = 512 × 512 × 100, field of view (FOV) = 240 × 240 × 100 mm, slice thickness = 0.8 mm, and number of acquisitions = 1. The nominal voxel resolution was 469 × 469 × 800 μm. The total acquisition time was 31 min. The acquisition of MR

images from one brain was also performed in a 7.0-Tesla, 40-cm bore magnet (magnet; KOBELCO and JASTEC, Japan, console; Bruker Biospin, Germany) interfaced to a Bruker-Avance I system using a 200-mm inner-diameter volume coil for transmission and reception coil (Rapid Biomedical, Germany). Sample temperature was maintained at room temperature ( $23 \pm 0.5$  °C) using a gradient coil cooling system (Bruker Biospin) and air-conditioners. The 3D images were obtained using a rapid acquisition with relaxation enhancement (RARE) sequence with the following parameters: TR = 300 ms, TE = 15.6 ms, rare factor = 2, matrix size =  $364 \times 272 \times 256$ , FOV =  $103.8 \times 77.5 \times 72.6$  mm, and number of acquisitions = 4. The nominal voxel resolution was  $285 \times 285 \times 285$   $\mu\text{m}^3$ . The total acquisition time was 11 h 36 m. The MR imaging data were reconstructed and analyzed using ParaVision software (Ver. 5.1, Bruker Biospin) and Osirix (Ver. 3.9.4, 64 bit, Pixmeo, Switzerland). Medical Image Processing, Analysis and Visualization (MIPAV) V7.2 software (National Institutes of Health Center for Information Technology, CIT) was used to re-orient the MR images from horizontal to sagittal and coronal planes. The final image data were adjusted in brightness and contrast using Photoshop (Adobe, San Jose, CA, USA) and assembled using Adobe Illustrator 10. Calculation of lobular volume fraction was done in a sample that was fixed in formalin for 6 months.

Lobules were identified by visualizing the surface of the cerebellum and examining serial MR images referencing Schmahmann et al. (1999), and Larsell and Jansen (1972).

#### *Macaques (Japanese monkey, Macaca fuscata)*

One adult Japanese macaque brain (courtesy of Drs. Takafumi Minamimoto and Arata Oh-Nishi) was perfused with 0.01 M phosphate-buffered saline (PBS; 150 mM NaCl, 10 mM sodium phosphate, pH = 7.4) and fixed with 4% paraformaldehyde. After post-fixation with 4% paraformaldehyde for two weeks, the cerebellum was dissected from the skull and soaked for 30 days in a 10 mM of phosphate buffer with 30% of sucrose and 0.1% of sodium azide. The brain was frozen at  $-80$  °C until use. The arachnoid was removed from the cerebellar surface and the brain surface was subsequently photographed to show lobular arrangements with a digital camera as described above. The acquisitions of MR images were performed in a 7.0-Tesla, 20-cm bore magnet (Biospec Avance-III, Bruker Biospin, Germany) using an 86-mm inner-diameter volume coil for transmission (Bruker Biospin) and a 35-mm 4-ch phased array coil for reception (Rapid Biomedical, Germany). Sample temperature was maintained at room temperature ( $23 \pm 0.5$  °C) using a gradient coil cooling system (Bruker Biospin) and air-conditioners. The 3D images were

obtained using a RARE sequence with the following parameters: TR = 300 ms, TE = 19.2 ms, rare factor = 4, matrix size =  $256 \times 256 \times 256$  or  $335 \times 240 \times 224$ , FOV =  $30 \times 30 \times 44.8$  or  $42 \times 30 \times 28$  mm, and number of acquisitions = 10. The nominal voxel resolution was  $117 \times 117 \times 175$  or  $125 \times 125 \times 125$   $\mu\text{m}$ . The total acquisition time was 13 h 39 m or 11 h 12 m. The MR imaging data were reconstructed and analyzed using ParaVision and Osirix. The MIPAV software was used to examine serial MR images for drawing and data annotation (using Adobe Illustrator 10).

#### *Marmosets (Callithrix Jacchus)*

One marmoset brain, which was perfused with phosphate-buffered saline, fixed with 4% paraformaldehyde for seven days (Fujita et al. 2010), soaked in 30% sucrose plus phosphate buffer (10 mM, pH 7.4) and stored in the deep freezer, was defrosted. The cerebellum was dissected and the arachnoid was removed from the cerebellar surface. The brain was soaked in 0.5% of phenol red in PBS for 10 min to produce an orange color at the orifice of the fissures, trapping the phenol red solution, to distinguish each folium. Then, the brain was soaked in PBS and imaged with an Olympus MVX10 macrozoom microscope equipped with a DP70, Olympus CCD camera.

The expression pattern of aldolase C, a marker for a subset of adult Purkinje cells (Hawkes and Leclerc 1987; Sugihara and Shinoda 2004), and axonal projections in the marmoset cerebellum were obtained from our previous study (Fujita et al. 2010) for the purpose of re-analysis applicable to the current study. Specifically, Purkinje cell axons originating in crus I or II were labeled with dextran amine conjugated with Texas red or tetramethyl rhodamine to examine their terminations in the posterior interposed nucleus. In addition, collateral climbing fibers labeled by injecting biotinylated dextran amine (BDA) into crus II were remapped sagittally by measuring the position of the labeled climbing fiber along the rostrocaudal direction from serial coronal sections as done previously (Quy et al. 2011).

The 3D model of the marmoset cerebellum reconstructed in our previous study (Fujita et al. 2010) was used to examine lobular organization transecting sagittal and horizontal planes using Rhinoceros, three-dimensional graphics software (Robert McNeel & Associates, Seattle, WA, USA.).

#### *Rats*

Three adult Long–Evans and one Wistar rats (Kiwa Laboratory Animals, Wakayama, Japan) were anesthetized

with sodium pentobarbiturate and perfused with 5% of paraformaldehyde. Brains were dissected from the skull and post-fixed for 24 h, after which they were soaked in 30% of sucrose for two days. Eighty-micron thick serial horizontal and sagittal sections were cut from two cerebellums, mounted on glass slide and stained with thionine to observe lobular morphology and calculate lobular volume fraction. To visualize the lobules from the cerebellar surface, one cerebellum was soaked in 0.5% of phenol red in PBS, rinsed in PBS, and then imaged with a macrozoom microscope as described above.

Five adult Long–Evans rats were used in experiments to label Purkinje cell axons with BDA. Experimental procedures were the same as described in our previous report (Sugihara et al. 2009). Briefly, a small amount (approximately 10 nl) of BDA (MW 3000, D-7135; Molecular Probes, Eugene, OR, 10% solution in saline) was injected into the molecular layer or Purkinje cell layer of crus I or crus II in rats under anesthesia with a cocktail of ketamine (130 mg/kg) and xylazine (8 mg/kg, intraperitoneal injection). Rats were perfused seven days after injection and 80- $\mu$ m thick serial coronal sections were cut. Sections were treated with avidin–biotin complex and 3-3'-diaminobenzidine (DAB) with nickel to visualize BDA-labeled axons in black. Subsequently, sections were incubated with biotinylated anti-aldolase C antibody followed by avidin–biotin complex and DAB to visualize aldolase C in brown (Sugihara and Shinoda 2004). The anti-aldolase C antibody was produced in our laboratory and its specificity in the rat cerebellum was tested with Western blot (Sugihara and Shinoda 2004). Entire axonal trajectories of seven Purkinje cells were reconstructed from crus I and crus II in the paravermal area (zone C2 or aldolase C stripe 4+//5+) in five rats according to previous reconstruction protocols (Sugihara et al. 2009). Three Purkinje cell axons from three rats of a previous study (Sugihara et al. 2009) were included for analysis. Thus, ten Purkinje cell axons were analyzed to understand the relationship between the lobule where the origin of axons was located (crus I or crus II) and their terminating target area within the posterior interposed nucleus. Single olivocerebellar axons reconstructed in our previous study (Sugihara et al. 2001) in rat were also examined for the purpose of this study. The pattern of climbing fiber axonal branching within cerebellar lobules (simple lobule, crus I, crus II, paramedian lobule and copula pyramidis) was analyzed in ten axons terminating in the paravermis and hemisphere.

### Mice

An adult ICR mouse (Clea Japan, Tokyo, Japan) and two C57BL/6N mice were anesthetized with sodium

pentobarbiturate and perfused with 4% paraformaldehyde. Brains were dissected from the skull and post-fixed for 24 h before soaking in 30% sucrose for two days. Eighty-micron serial horizontal and sagittal sections were cut from two C57BL/6N mouse cerebellums, mounted on glass slides for observation of lobular morphology and calculation of lobular volume fraction. To observe the lobules from the cerebellar surface, one ICR mouse cerebellum was soaked in 0.5% phenol red in PBS to obtain an orange color. Finally, the brain was rinsed in PBS and imaged with a macrozoom microscope as above.

Expression of aldolase C is labeled by fluorescent protein venus in the Aldoc-Venus mouse (Fujita et al. 2014). Therefore, epifluorescent images of the cerebellar surface of the Aldoc-Venus mouse from our previous study (Fujita et al. 2014) were edited for this study by focusing on the hemisphere and paravermal regions.

### Estimation of volume fraction of crus I/II

To estimate the volume fraction of a lobule of interest relative to the whole cerebellar volume we applied the Cavalieri method, by drawing contours of the whole cerebellum and the region of interest in several ( $n = 6–12$ ) sagittal (right side) and horizontal (coronal for human cerebellum) sections separated by similar intervals (MR images in the human and macaque cerebellum, transections of the 3D model in the marmoset cerebellum, histological sections in the rat and mouse cerebellum). These sections were chosen at similar intervals encompassing the whole cerebellum (for horizontal or coronal sections) or the right cerebellar hemisphere (for sagittal sections). Then, the entire cerebellum (or the right hemisphere) was divided into  $n$  horizontal (or coronal) or sagittal divisions. Division  $r$  was defined as the part of the cerebellum where the position was closer to section  $r$  than to other sections. Section  $r$  represented the section for the whole division  $r$ . Then, the volume fraction of the lobule of interest was calculated as  $LIV/WCV$ , where  $LIV$  and  $WCV$  represent the volume of the lobule of interest and volume of the whole cerebellum. The product of the sum of all cross-sectional areas of the region of interest together with the uniform intervals between regions provide an unbiased estimation of the volume of our region of interest. The volume estimate formulas are as follows:

$$\begin{aligned} WCV &= \sum_{r=1}^n (\text{Cerebellar volume in division } r) \\ &= \sum_{r=1}^n \{ (\text{Thickness of division } r) \\ &\quad \cdot (\text{Area of the cerebellum in section } r) \}, \end{aligned}$$



$$\begin{aligned} \text{LIV} &= \sum_{r=1}^n (\text{Volume of the lobule of interest in division } r) \\ &= \sum_{r=1}^n \{(\text{Thickness of division } r) \\ &\quad \cdot (\text{Area of the lobule of interest in section } r)\}. \end{aligned}$$

Finally, the average of the volume fraction of the lobule of interest (LIV/WCV) estimated from sagittal and horizontal sections were calculated.

In human, measurements were done in seven sagittal and six coronal sections of the re-oriented MR images. In macaque, measurement was done in 8 sagittal and 12 horizontal slices of MR images. In marmoset, ten sagittal and eight horizontal sections were obtained by cutting the three-dimensional reconstruction of the marmoset cerebellum (Fujita et al. 2010). Since this reconstruction represents the Purkinje cell layer, the molecular layer was drawn manually. In rat (Long–Evans strain, two adult samples) and mouse (C57BL/6N strain, two adult samples), estimation was obtained from 7 to 8 sagittal and horizontal sections. The shrinkage factor of the brain was comparable across the processed brains because all brains were fixed using aldehydes with similar cross-linking properties (10% formalin is roughly 4% formaldehyde with methanol added, and 4–5% paraformaldehyde solution contains 4–5% formaldehyde) for a comparable amount of time. Although the shrinkage factor of the brain may not have been identical among brain samples due to the use of somewhat different fixation protocols, the shrinkage factor was not supposed to affect the measured volume fraction because the volume fraction of a lobule was normalized to the volume of the whole cerebellum in each brain sample. Besides, our volume calculation in human was comparable to that of Balsters et al. (2010).

### Cerebellar lobules as a common landmark of cerebellar organization in mammals

Genetic mechanisms in the developing cerebellum enable correct migration of granule cell precursors that give rise to lobulation (Sudarov and Joyner 2007). Lobular organization of the cerebellum is highly conserved among individuals of the same animal species, and well conserved between phylogenetically close animal species such as rats and mice (Paxinos and Franklin 2001; Sugihara and Quy, 2007). The major lobulation pattern in adult mammals and the developmental appearance of major fissures, which separate individual lobules, are similar across various mammalian species (Larsell 1937, 1970; Larsell and Jansen 1972). In addition, the developmental origin of the cerebellar hemisphere derives from the alar plate of rhombomere (r) 1, whereas that of the vermis derives from r0 or

isthmus (Martinez et al. 2013; communication with Luis Puelles). The difference in origins of individual lobules in the vermis or hemisphere remains to be explored.

Similarly, the functional localization of cerebellar lobules is observed across various mammalian species. For example, adaptation of reflexive eye movements is controlled by the flocculus (monkey: Lisberger and Fuchs 1978; cat: Sato and Kawasaki 1984; rabbit: Ito et al. 1977; mouse: Koekkoek et al. 1997), and signals that are related to the adaptation of walking are recorded in vermis lobules III–V (mouse: Ozden et al. 2012; ferret: Lou and Bloedel 1992; human: Jahn et al. 2008).

It is to be noted that location of the function that is related to each individual lobule does not match exactly the individual folia of each lobule. For example, the vestibular system-related activities that characterize the nodulus (vermal lobule X) is not only located in the nodulus but also in part of the uvula (lobule IX) that neighbors the nodulus (Barmack et al. 1992). This functional versus anatomical mismatch may further be highlighted by the terminal distribution area of single mossy or climbing fiber axons, which are not exactly parceled into an individual lobule but rather innervating multiple lobules (Wu et al. 1999; Quy et al. 2011; Sugihara and Shinoda 2004; Sugihara et al. 2004; Pijpers et al. 2006).

Nevertheless, the afferent and efferent projection pattern of axons are highly correlated with lobular organization of the cerebellum as axons consistently branch to and converge from specific preferred lobules (Quy et al. 2011; Fujita and Sugihara 2013). The pattern is also highly correlated with the longitudinal organization of the cerebellar cortex represented by spatial arrangements of Purkinje cell subsets that express a specific profile of molecules including zebrin (Voogd et al. 2003; Sugihara and Shinoda 2004; Pijpers et al. 2006). The zebrin pattern, in turn, is uniquely correlated with the lobular organization whereby the striped pattern in each lobule is not exactly the same as the pattern in other lobules (Fujita et al. 2014). In the rostral-caudal plane, the lobules are classified into four groups (anterior, central, posterior, and nodular zones) that show strikingly distinct zebrin-striped patterns (Hawkes and Leclerc 1987; Ozol et al. 1999). Excitability of Purkinje cells and synaptic plasticity are different across different lobules (Kim et al. 2012), which may be related to lobule-dependent zebrin-striped patterns (Wadiche and Jahr 2005). Although the boundary of the four groups of zebrin patterns does not exactly match in the bottom of the fissures which separate the lobules, the positional relationship between the major zebrin stripes and the lobular organization is conserved nearly in the entire mammalian cerebellum, including rat, mouse and marmoset (Fujita et al. 2010, 2014), and in a wider variety of mammals at least in the vermal anterior lobe (Sillitoe et al. 2005; Marzban and Hawkes 2011).

As a whole, cerebellar lobules have consistent positional relationship with axonal projection patterns and zebrin-stripped patterns that are conserved among mammals. This indicates that cerebellar lobules are potentially landmark structures relating comparative aspects of anatomical and physiological properties of the cerebellum. Consequently, it is essential to identify homologous lobules across mammalian species.

### Anatomical definition of crus I and crus II and their neighboring lobules

Crus I and crus II of the ansiform lobule are the names that originate from Bolk's monograph (1906). He traced sequential axis of cerebellar foliation in lemur and other mammals from the rostral end to the caudal end. The single sequential axis in the anterior lobe is divided into the vermal and hemispheric sequential axes in the posterior lobe. In the area caudal to the simple lobule or lobule VI of Larsell (1952, 1953, 1970), the hemispheric sequential axis extends laterally (crus I) and returns medially (crus II) by making a loop (ansiform lobule) to the paramedian area (paramedian lobule) and curved laterally again toward the ventrolateral direction (paraflocculus and flocculus). Thus, the ansiform lobule which protrudes laterally in the central cerebellum is subdivided into rostral and caudal parts (crus I and crus II, respectively), although the boundary between crus I and crus II has not been clearly defined. The nomenclature of crus I and crus II was adopted by Larsell in his detailed description of lobular structure observed mainly from the cerebellar surface in rat, cat, rhesus monkey (Larsell 1952, 1953, 1970) and human (Larsell and Jansen 1972), while he introduced roman numerals I–X to define the vermal lobules.

In the human cerebellum, superior and inferior semilunar lobules (Nieuwenhuys et al. 2008) are the conventional nomenclature for the lobules that were defined as crus I and crus II by Larsell and Jansen (1972). Schmähmann et al. (1999) applied Larsell's nomenclature in human cerebellum for MR imaging of human cerebellum. There are no obvious discrepancies in defining crus I and crus II (or superior and inferior semilunar lobules) in the literature about the human cerebellum. It is presumably because of the presence of the horizontal fissure as a landmark, which borders crus I and crus II, the two lobules that are extended most laterally in cerebellar hemispheres.

In the macaque and marmoset cerebellum, Larsell's definition of crus I and crus II was not consistently followed in later literature as summarized in the next section (Larsell/Brodal-type and Paxinos-type definitions).

In the rat cerebellum, Larsell (1952, 1970) made a detailed observation of the lobular structure from the

surface of the cerebellum and defined all major lobules. His definition of crus I and crus II is reflected in all major atlases (Paxinos and Watson 2007; Swanson 1998). The lobular structure in the mouse cerebellum (Marani and Voogd 1979; Paxinos and Flanklin 2001) is similar to that in the rat cerebellum. There are no discrepancies in the definition of crus I and crus II in literature with regards to rat and mouse.

The hemispheric lobule that is located rostral to crus I is designated as the "simple lobule" (Bolk 1906; Larsell 1953; Madigan and Carpenter 1971; Paxinos et al. 2000, 2011; Voogd 2004) or "hemispheric lobule VI (HVI)" (Larsell 1970; Schmähmann et al. 1999). Although "simple lobule" was initially used to indicate both the vermal and hemispheric parts of rostral lobule VI by Bolk (1906) due to the lack of paravermal fissure in this area, this term is used to indicate the hemispheric part that extends from vermal lobule VI (Larsell 1953). The hemispheric lobule that is located caudal to crus II is designated as the "paramedian lobule" (Bolk 1906; Larsell 1953; Madigan and Carpenter 1971; Paxinos et al. 2000, 2011; Voogd 2004) or "hemispheric lobule VIIIB (HVIIIB)" (Larsell 1970; Schmähmann et al. 1999). This lobule is the lateral extension of the caudal sublobule of vermal lobule VII (VIIIB) in human and macaque. HVIIIB may be used in rodent cerebellum in analogy to that in macaque even though there are no sub-lobules in vermal lobule VII (Larsell 1970). The lateral extension of lobule VIII is designated as the "posterior part of the paramedian lobule" (Larsell 1953; Madigan and Carpenter 1971), "copula pyramidis" (Larsell 1970; Paxinos et al. 2000, 2011; Voogd 2004) or "HVIIIA" (Schmähmann et al. 1999). In this review, we adopt the nomenclature used in the human cerebellum HVI, HVIIIB and HVIIIA when indicating to neighboring lobules across animal species.

### Inconsistency in definitions of crus I and crus II in the non-human primate cerebellum

Larsell's monograph (1970), which contains more detailed observations compared to his original paper (Larsell 1953), shows the outer view of the rhesus monkey cerebellum from various aspects with definitions of individual lobules. In all his outer view drawings of the cerebellum, the lobule that was defined as crus I is the lobule that is extended most laterally (orange area in Fig. 1a) while the lobule that was defined as crus II (light blue area in Fig. 1a) is located caudoventrally to crus I and much less extended laterally compared to the lobule defined as crus I. Anatomical studies of rhesus monkey cerebellum by Brodal (1979) designated crus I and crus II in the same way as Larsell; the term crus I was used to indicate multiple folia that occupy

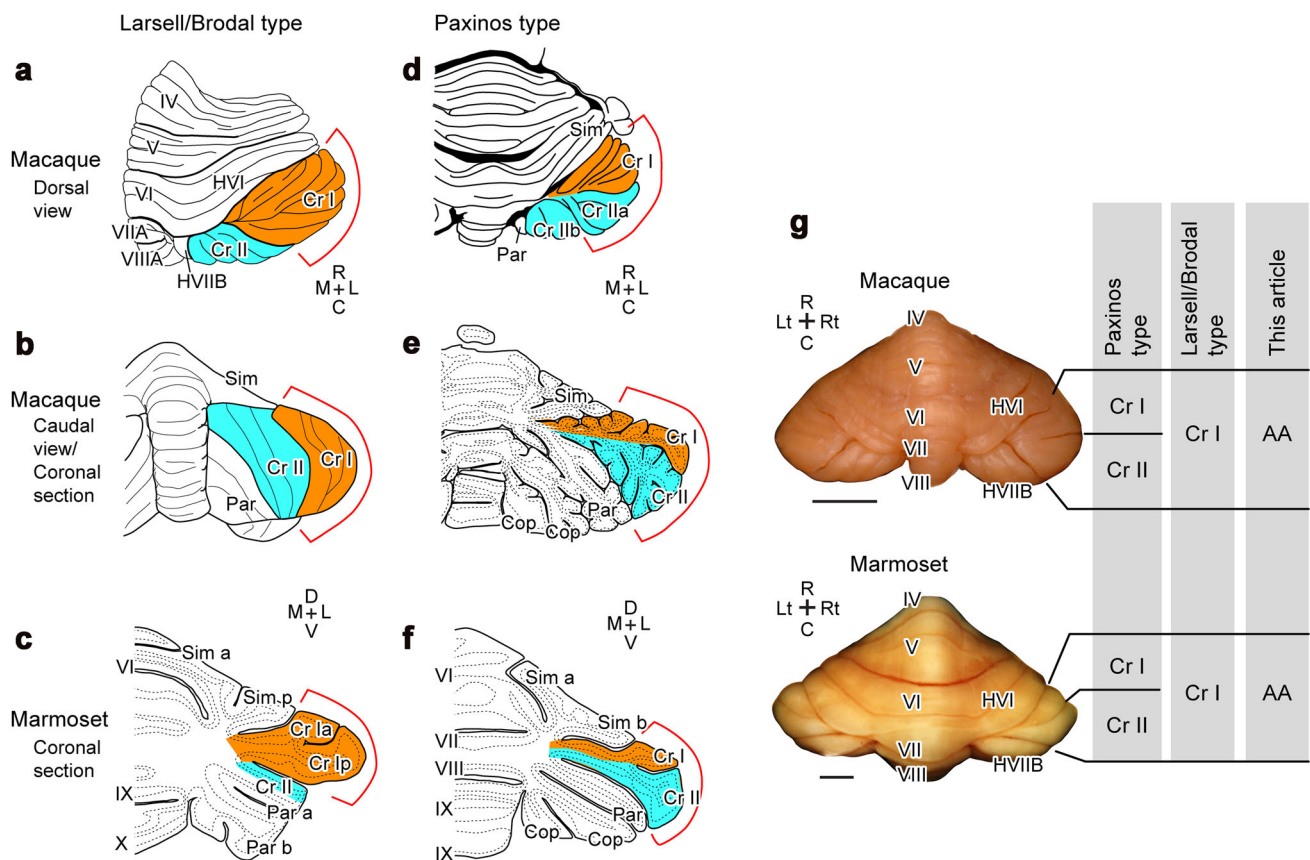


**Fig. 1** Discrepancy in defining crus I and crus II in non-human primate cerebellums. **a–f**, Crus I and crus II defined in several articles in rhesus monkey and marmoset. The *left column* shows Larsell/Brodal’s definition of crus I and II (**a–c**), while the *right column* shows Paxinos’ definition (**d–f**). The region circumscribed by the *red contour* indicates the homologous lobule that is designated as the “ansiform area (AA)”. Drawings were reproduced from Fig. 181 of Larsell (1970) (**a**), Fig. 5 of Brodal (1979) (**b**), Fig. 2e of Fujita et al. (2010) (**c**), Fig. 2 of Madigan and Carpenter (1971) (**d**), Fig. 133 of Paxinos et al. (2000) (**e**) and Figure MA1#53 P7.0 of Paxinos et al. (2011) (**f**). **g** Photos of the dorsal aspects of macaque (Japanese

monkey, *top*) and marmoset (*bottom*) showing two types of definitions of crus I and crus II. Names for visible vermal lobules (IV, V, VI, VII and VIII) and hemispheric lobules (HVI and HVIIB, refer to Table 1 for different nomenclatures) are provided. The flocculus, paraflocculus and brainstem were trimmed for clarity. *Brightness and contrast* of photos were adjusted with Adobe Photoshop. *Scale bars* 10 mm (*top*), 2 mm (*bottom*). *IV–X* lobule IV–X, *a* sublobule a, *AA* ansiform area, *b* sublobule b, *C* caudal, *Cop* copula pyramidis, *Cr I* crus I, *Cr II* crus II, *D* dorsal, *H* hemispheric, *L* lateral, *Lt* left, *M* medial, *p* sublobule p, *Par* paramedian lobule *R* rostral, *Rt* right, *Sim* simple lobule, *V* ventral

the entire laterally-expanded part of the hemisphere (Fig. 1b). Therefore, here, we designated this type of definition of crus I/II as Larsell/Brodal’s type. In the atlas of the macaque cerebellum by Madigan and Carpenter (1971), the lobules (or combined folia) that are extended most laterally were defined as crus I, which is similar to Larsell’s definition, in horizontal and sagittal sections. However, coronal sections by Madigan and Carpenter (1971) support a different definition of crus I and crus II in that the lobule which extends most laterally (defined as crus I in horizontal and sagittal sections) is divided into two parts by the central fissure: (1) the rostral and (2) caudal parts of which have been defined as crus I and crus IIa, respectively (Fig. 1d). In the atlas of the macaque brain by Paxinos et al. (2000), which contains only coronal sections, the lobule or the combination of folia that are extended most laterally has also been divided into crus I and crus II

(Fig. 1e). In this review, we designate this type of definition of crus I/II as Paxinos type. Recent publications about the monkey cerebellum are seen to adopt the Paxinos-type definition (Kelly and Strick 2003; Glickstein et al. 2011). It is not clear why the definition of crus I and crus II was changed in the monkey cerebellum. One possibility is that the summary schematic of the unfolded cerebellum by Larsell (1970), which depicted both crus I and crus II in the most laterally-extended part of the hemisphere, and the analogy to human cerebellum crus I and crus II, both of which are extended laterally in the hemisphere, affected later definitions.

A similar inconsistency in the definition of crus I and crus II exists in marmoset articles. The marmoset cerebellum has a lobular organization which is similar to but simpler than that of the macaque cerebellum. We defined crus I and crus II according to the Larsell/Brodal-type

**Table 1** Comparison between the nomenclature in the present study and nomenclatures in the literature for homologous hemispheric lobules in human, macaque, marmoset, and rodents (rat and mouse)

This article	Paxinos-type nomenclature		Larsell/Brodal-type nomenclature			Rat/mouse
	Macaque	Marmoset	Macaque	Marmoset	Marmoset	
Schmahmann et al. (1999)	Madigan and Carpenter (1971) dorsal surface drawing (Fig. 2) and transverse section series	Paxinos et al. (2000)	Larsell (1953)	Paxinos et al. (2011)	Madigan and Carpenter (1971) sagittal section series and horizontal section series; Brodal (1979)	Larsell (1970) (Albino rat chapter) and others <sup>a</sup>
HVI	Sim	Sim	Sim	Sim	Sim	Sim/HVI
AA	crus I	crus I	crus I	crus I	crus I	crus I
	+	+				
	crus II	crus II				
HVIII	crus IIa	crus II	crus II	crus II	crus IIa	crus II
	crus IIp	Par	+	+	+	+
			Par a	HVIII	crus IIp	Par
HVIII	Par	Cop	Par p	HVIII	Par	Cop
			Par p	HVIII	Par p	Cop
					(Cop)	

a, A, B, p sublobule a, A, B, p, AA ansiform area, Cop copula pyramidis, Par paramedian lobule, Sim simple lobule

<sup>a</sup> Paxinos and Watson (2007), Voogd (2004), Paxinos and Franklin (2001), Fujita et al. (2014)



definition in our analysis of the marmoset cerebellar organization (Fujita et al. 2010; Fig. 1c). However, the atlas of the marmoset brain by Paxinos et al. (2011) has defined crus I and crus II according to the Paxinos-type definition (Fig. 1f). The differences in these definitions are evident in the coronal sections reproduced from these articles (Fig. 1c, f). Besides definitions of lobule names, however, structure of the cerebellar lobular organization in marmoset (Fig. 1c, f) is similar to that in macaque (Fig. 1e) and in squirrel monkey (Fig. P7.5 of Emmers and Akert 1963). The identical lobule indicated by the red curve is defined differently between Fig. 1c and f (only crus I in Fig. 1c but separated into crus I and crus II in Fig. 1f). The discrepancies in the definition of crus I and crus II of macaque and marmoset is summarized in a part of Table 1.

In our study of the organization of the marmoset cerebellum (Fujita et al. 2010) we argued that crus I and crus II in the marmoset (Larsell/Brodal-type definition) and rat were homologous based on several aspects. However, taking the Paxinos definition into account, crus I and crus II in the marmoset may not be homologous to those same lobules in the rat. Since such inter-species inconsistency was also previously indicated in the vermal lobules VI–VII between marmoset and rat (Fujita et al. 2010), we made a careful and systematic comparison of the lobular structure in the crus I/II area in human, macaque (Japanese monkey), marmoset, rat and mouse cerebellums. Because of the inconsistencies in the definitions of crus I and crus II among human, non-human primates and rodents, we need a term that designates the homologous crus I/II area across animals. Thus, in this article, we utilized the term “ansiform area (AA)” to refer to the region that is extended most laterally and identified as both crus I/II in human (Paxinos definition in non-human primates) or only crus I in rat/mouse (Larsell/Brodal-type definition in non-human primates) (Table 1).

### External structures reveal inter-species ansiform area homology

Comparison of external structures in the cerebellar hemisphere of human, non-human primate and rodent revealed a striking lobular homology leading us to suggest the use of the term ansiform area (AA) to indicate homologous lobules in this region across these species. First, our results demonstrated that in the postero-inferior aspect of the human cerebellum (equivalent to the dorso-caudal aspect of the animal cerebellum), crus I/II emerged from the paravermal area and expanded in the hemisphere revealing the AA (Fig. 2a1–3, encircled by dashed lines). Conversely, neighboring lobules VI and VIIIB of the cerebellar hemisphere (abbreviated as HVI and HVIIIB, respectively, Schmahmann et al. 1999) were continuous with lobules VI and VIIIB of the vermis in the human

cerebellum. Second, in the dorso-caudal aspect of the macaque cerebellum, emergence of the lobule equivalent to human crus I/II (AA) from the paravermal area was identified between the neighboring rostral HVI lobule and caudal HVIIIB lobules (Fig. 2b1–3, arrowheads and encircled by dashed lines). Third, in the dorso-caudal aspect of the marmoset cerebellum, the lobule equivalent to the macaque AA (Fig. 2b) emerged from the paravermal area (Fig. 2c1–3, arrowheads) and extended toward the hemisphere (Fig. 2c1–3, encirclement by dashed lines), while the neighboring rostral HVI lobule and caudal HVIIIB lobules were continuous with the vermis (Fig. 2c). Fourth, in the dorso-caudal aspect of the rat and mouse cerebellums, the lobule equivalent to the marmoset AA (Fig. 2c) emerged from the paravermal area, with a narrow bridge-like connection to the vermis (Fig. 2d1–3, e1–3, arrowheads), extending toward the hemisphere (Fig. 2d1–3, e1–3, encirclement by dashed lines), while the neighboring rostral HVI lobule and caudal HVIIIB lobules were directly continuous with the vermis (Fig. 2d, e). Lastly, in all animal species examined, the AA expanded in the lateral hemisphere and occupied the hemispheric lateral pole (Fig. 2). Therefore, the AA in non-human primates and rodent cerebellums as designated here appears to be equivalent to crus I/II in the human cerebellum (Fig. 2). However, the AA is designated differently across species. In humans, crus I/II is equivalent to the AA, whereas in non-human primates either crus I/II or only crus I reflects the AA (Fig. 1). Finally, in rodents, only crus I reflects the AA (Larsell 1970; Paxinos and Watson 2007; Paxinos and Franklin 2001). Morphological characteristics of the outer shape of the AA are summarized as follows in the human, primate and rodent cerebellums: (1) the AA is located roughly in the central cerebellum in the rostrocaudal axis, (2) the AA emerges from the paravermis at the rostrocaudal level of rostral lobule VII or caudal lobule VI and expands toward the lateral pole of the hemisphere, and (3) the AA has a radiating foliation pattern, with a small number of folia in the medial part and a large number of folia in the lateral part (Figs. 2 and 4). The folia in the lateral part of the AA may be grouped into the rostral and caudal folia corresponding to crus I and crus II in human, and crus Ia and Ib–c in rodents. Correspondence between nomenclature in this review and nomenclatures in previous reports is provided in Table 1.

### Folia pattern further demonstrates ansiform area homology

Examination of human, non-human primate and rodent folia pattern in horizontal, coronal (human) and sagittal cerebellar tissue sections supported that the AA showed homology among species. The main observation was the AA's separation from neighboring lobules by deep fissures

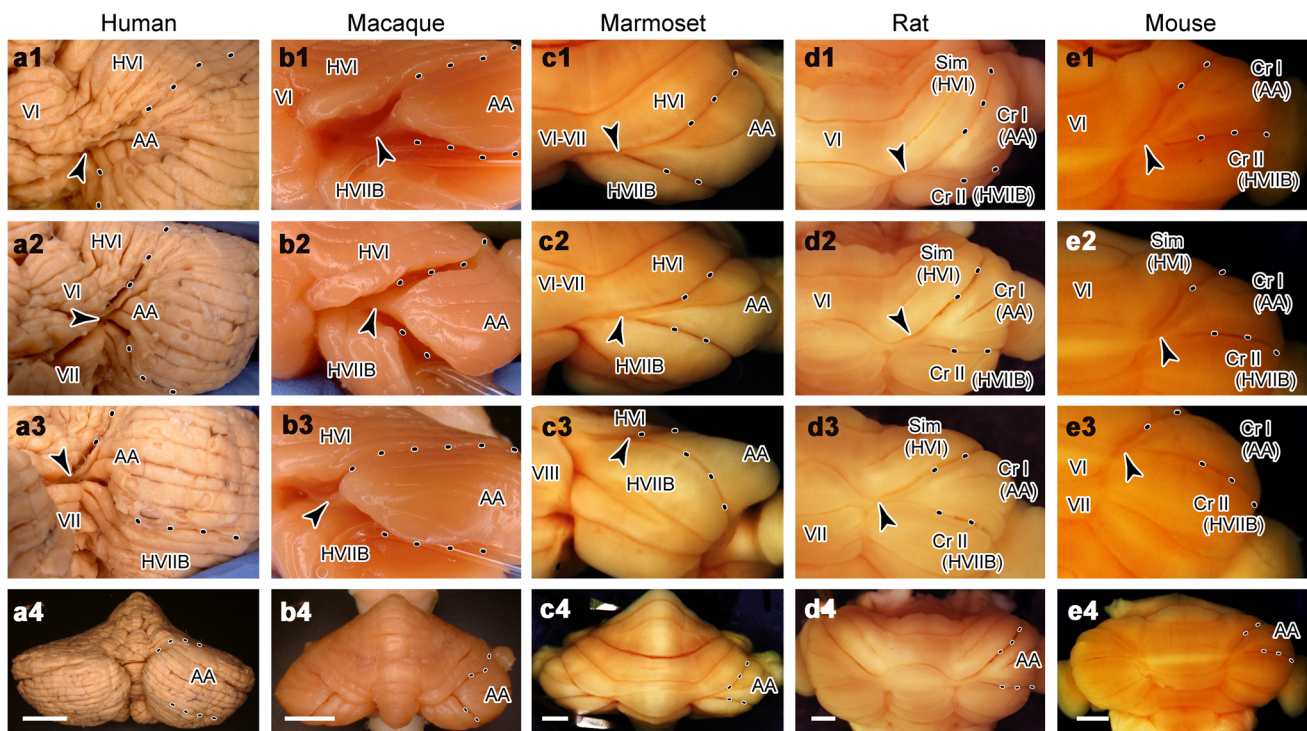


**Fig. 2** Lobulation pattern in the dorsal (posterior in human) aspect of the cerebellum in human (**a1–a4**), macaque (Japanese monkey) (**b1–b4**), marmoset (**c1–c4**), rat (**d1–d4**) and mouse (**e1–e4**). The *right* AA, which is equivalent to crus I in rodents and to crus I/II in human is encircled by dashed curves. The *top three photos* in each column show magnified views of the cerebellum focused on the rostral, center and caudal boundary of the AA (1, 2 and 3, respectively). The *bottom photos* (**a4**, **b4**, **c4**, **d4** and **e4**) in each *column* show the dorsal (animals) or caudal (human) aspect of the entire cerebellum to

demonstrate the relative position of the AA. The *arrowheads* indicate the most medial corner of the AA. Standard lobule nomenclature for human cerebellum (Schmahmann et al. 1999) was adopted for macaque and marmoset. The proposed consistent nomenclature is shown in parenthesis for rat and mouse. *Scale bars* in the *bottom panels*, 20 mm (**a4**), 10 mm (**b4**), 2 mm (**c4**), 1 mm (**d4** and **e4**). VI lobule VI, VII lobule VII, AA ansiform area, Cr I crus I, Cr II crus II, HVI hemispheric lobule VI, HVIIB hemispheric lobule VIIIB, Sim simple lobule

and its arrangement in the same positional relationship with neighboring lobules (orange areas in Fig. 3). However, to confirm this homology, we inquired as to whether characteristic similarities existed in the foliation pattern of the AA across species. To do this, we examined multiple cerebellar sections of human, macaque and marmoset.

In the human cerebellum (Fig. 4), the AA or crus I/II emerged from the paravermal area between lobules VI and VIIIB and showed an increase in size in the more lateral levels of the hemisphere (Fig. 4f). Although the horizontal fissure separated crus I and crus II, the posterior superior fissure between lobule HVI and crus I, and the ansoparamedian fissure between lobules crus II and HVIIB were deeper as characterized by being closer to the cerebellar white matter deep in the cerebellum compared to the horizontal fissure at all sagittal and horizontal levels (Fig. 4a–f). Therefore, based on these observations of fissure depths, we included both crus I and II into the AA. Taken together, lobules III, IV–V, VI, crus I/II (AA), VIIIB, VIII are the six major lobules in the hemisphere separated by deep fissures in the human cerebellar hemisphere (Fig. 4b, e). Similar

results were observed in two other human samples that we studied with MR imaging (data not shown).

In sagittal and horizontal sections of the marmoset (3D scheme, Fujita et al. 2010) and macaque cerebellum (MR images, Fig. 5h), identification of the lobule homologous to the human AA was revealed by several methods. Using three-dimensional analysis, we first confirmed that the AA in marmoset and macaque sections (Fig. 5a–g, orange areas) were identical to the lobules demarcated as AA in the whole mount preparation (Fig. 2). We then observed that (1) the AA (crus I/II in Paxinos definition or crus I in Larsell/Brodal definition) occupied the lateral pole of the hemisphere (Fig. 5a, b) that (2) the AA was separated from the neighboring rostral and caudal lobules by deep fissures (Fig. 5a, f), and (3) the AA was the fourth lobule from the rostral end among the major lobules in the hemisphere (III, IV–V, VI, AA, VIIIB and VIII) (Fig. 5a, b, f). These observed characteristics for the AA in marmoset and macaque cerebellar sections were the same as those for the AA in human cerebellar sections. These results indicate that we identified a homologous lobule, the AA, in human, macaque and marmoset cerebellums.

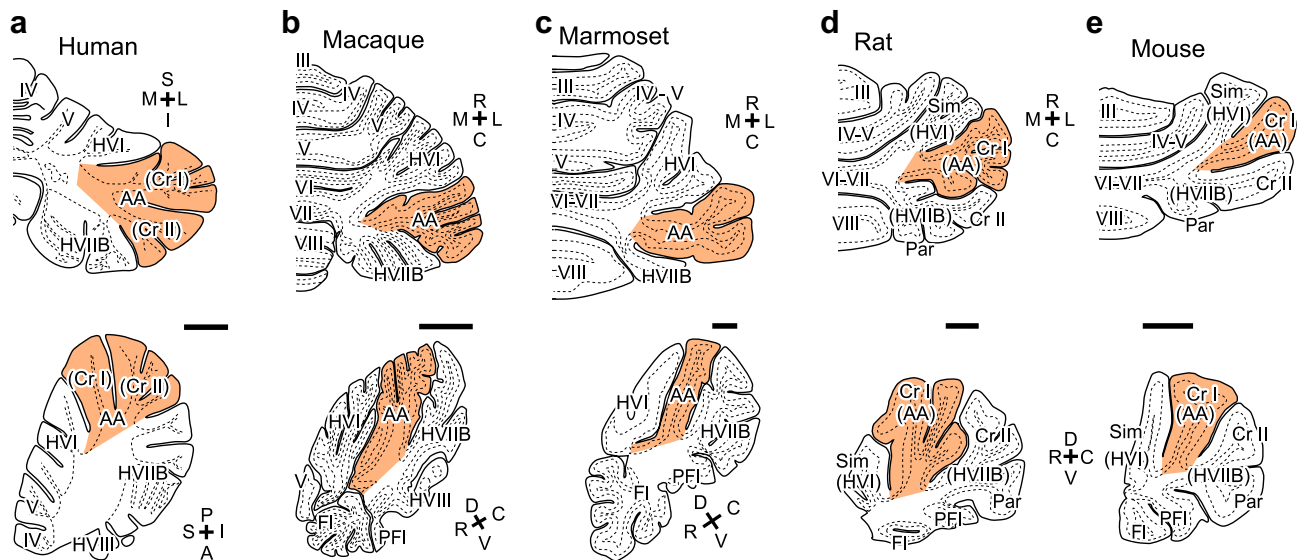


**Fig. 3** Comparison of the AA from human (**a**), macaque (**b**), marmoset (**c**), rat (**d**) and mouse (**e**) in *horizontal (right half) and sagittal cerebellar sections*. The AA is colored orange in drawings of representative *sagittal and horizontal sections*. **d** (rat) and **e** (mouse) use conventional lobule names with the standard lobule names indicated in *parentheses*. A coronal section is shown in human (**a**, top) in place of the *horizontal section*. Refer to Table 1 for

correspondence between nomenclatures in this figure in present and previous studies. *Scale bars* 10 mm (**a**), 5 mm (**b**), 1 mm (**c–e**). *III–X lobule III–X, A anterior, AA ansiform area, B sublobule B, C caudal, Cr I crus I, Cr II crus II, D dorsal, Fl flocculus, H hemispheric, I inferior, L lateral, Lt left, M medial, P posterior, Par paramedian lobule, PFI paraflocculus, R rostral, Rt right, S superior, Sim simple lobule, V ventral*

Based on the lobular definition from previous reports in rodent cerebellums (rat, Larsell 1970; Voogd 2004; Paxinos and Watson 2007; mouse, Paxinos and Franklin 2001; Fujita et al. 2014), we concluded that the lobule defined as crus I in rodents was homologous to the AA in other animals. In the rat and mouse, crus I (or the AA, Fig. 2d, e) was separated from neighboring rostral and caudal lobules by deep fissures and occupied the most lateral part of the hemisphere (Fig. 3d, e; also refer to figures in Larsell 1970; Voogd 2004; Paxinos and Watson 2007; Paxinos and Franklin 2001; Fujita et al. 2014). In addition, crus I (or the AA) consisted of only one folium in the medial part, but was divided into multiple folia in the lateral parts (Fig. 3d, e). These characteristics in shape of crus I (or the AA) in rat and mouse indicate a high similarity in structure of the cerebellar hemisphere between rodents and non-human primates. Based on this similarity, the simple lobule, crus I, crus II, paramedian lobule, and copula pyramidis in the conventional nomenclature were thought to be equivalent to HVI, AA, rostral part of HVIIB, caudal part of HVIIB, and HVIII, respectively, in the rat and mouse cerebellums in this study (Fig. 3d, e; Table 1).

Thus, our analyses in horizontal and sagittal cerebellar sections indicated that the rodent AA is homologous to both human crus I and crus II lobules, and this homology is observed with consistency in the macaque, marmoset, rat and mouse cerebellum (Fig. 3).

In genetic studies using mice, *En1* and *En2* are involved in early development of the cerebellum (Joyner et al. 1991;

Martinez et al. 2013). Inactivation of *En1* and *En2* genes causes foliation defects in the vermis and hemisphere (Sgaiet et al. 2007). Whereas foliation defects of crus I (AA) are not obvious, separation of the folia between crus II and paramedian lobule is lost in cases in which *En2* gene is inactivated. This suggests that crus II is more akin to paramedian lobule than to crus I in mouse, supporting our identification of the AA (crus I) and neighboring HVIIB (rostral HVIIB = crus II, caudal HVIIB = paramedian lobule, in rodents, Table 1).

### Axonal projection patterns confirm distinction of the AA

To examine whether lobule-specific axonal connections are conserved in the AA across mammals, projection patterns of afferent and efferent axons of the cerebellar cortex should be examined. Projections of climbing fiber axons and Purkinje cell axons are topographically correlated primarily with the longitudinal striped pattern (zones C1, C2, C3, D1, D0 and D2; or aldolase C stripes) in the cerebellar cortex (Groenewegen et al. 1979; Buisseret-Delmas 1988; Buisseret-Delmas and Angaut 1989; Voogd et al. 2003; Sugihara and Shinoda 2004; Sugihara et al. 2009; Fujita et al. 2010). The projections of pontine nucleus axons, which are the main mossy fiber afferents in the crus I/II area (Brodal 1981) are also organized within longitudinal striped patterns (Serapide et al. 2001).



## Human

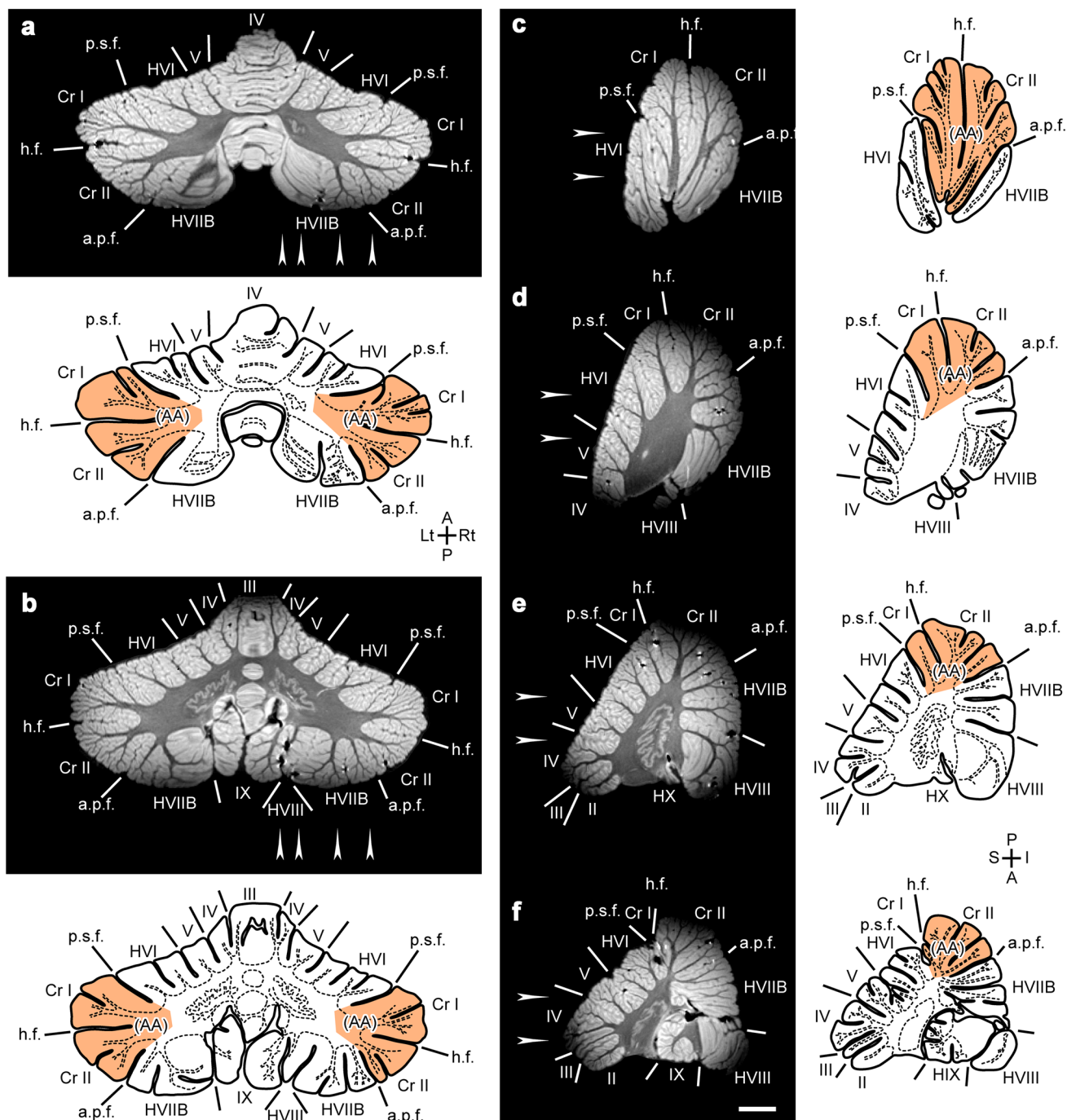


**Fig. 4** Coronal (equivalent to the *horizontal plane* in non-human primates and rodents) and *sagittal* sections from human cerebellum at different levels. Re-oriented 7.0-Tesla MR images and drawings of major lobules and fissures based on the digital images. The AA which is identical to crus I/II in human cerebellum is colored orange. The levels of *sagittal* and *coronal* sections are indicated with arrowheads

in **a** and **b**, and in **c–f**. Scale bar 10 mm. Small black spots with white flare in MR images are artifacts due to an air bubble. II–X lobule II–X, A anterior, AA ansiform area, a.p.f. ansoparamedian fissure, B sublobule B, Cr I crus I, Cr II crus II, H hemispheric, h.f. horizontal fissure, I inferior, P posterior, p.s.f. posterior superior fissure, S superior

Interestingly, the afferent and efferent projections are also topographically correlated with cerebellar lobules as shown in our previous studies of single climbing fiber axons

(Sugihara et al. 2001), and also in studies of projections of Purkinje cell axons and pontine mossy fiber axons performed with a variety of techniques in primates and rodents



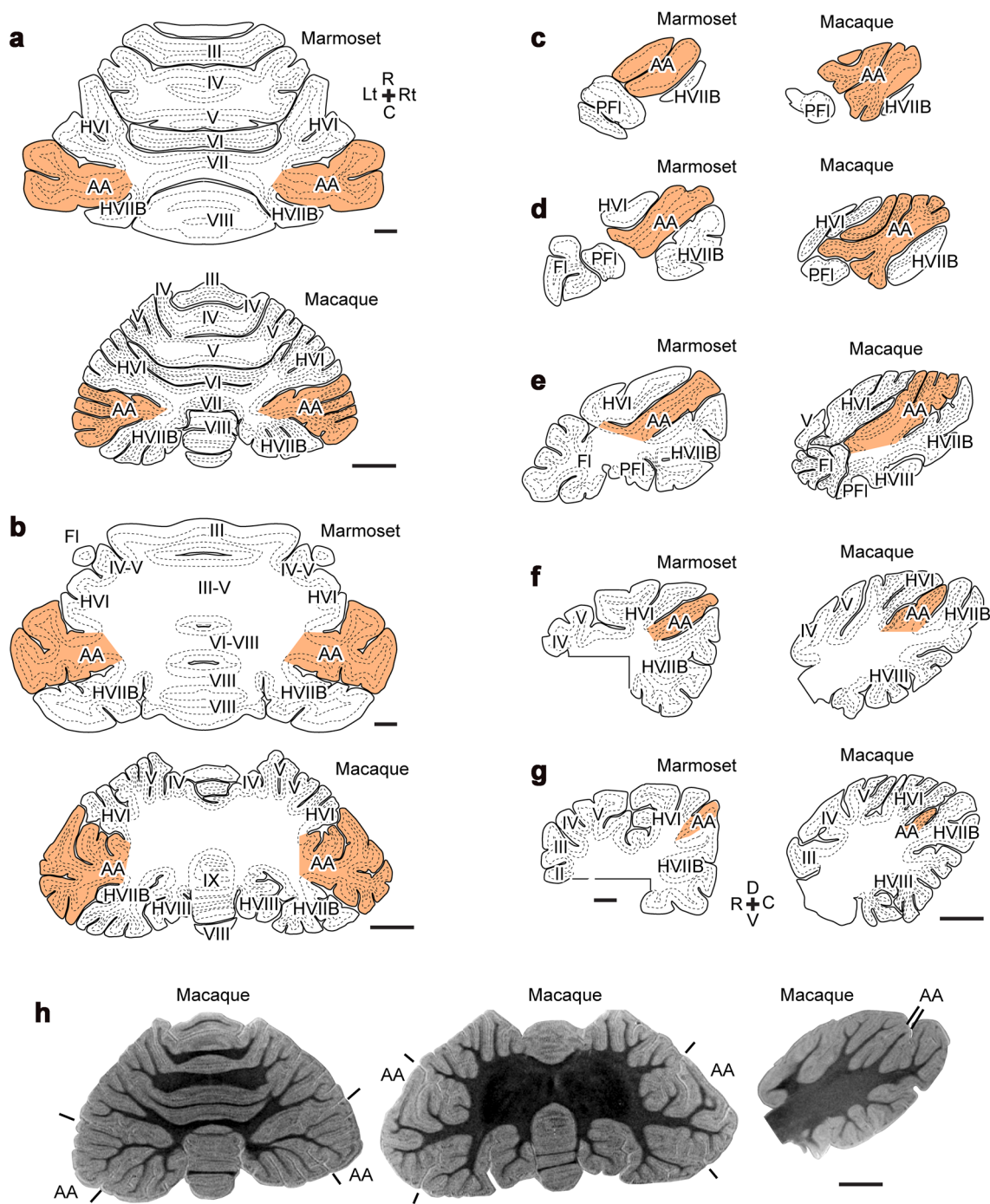


**Fig. 5** Horizontal and sagittal sections of the marmoset and macaque cerebellum at several different levels to show positions of the AA as defined in this paper. **a–g** Comparison of marmoset and macaque cerebellar sections at equivalent horizontal and sagittal levels. Marmoset cerebellar sections were obtained by cutting the three-dimensional model of the marmoset cerebellum constructed in our laboratory (Fujita et al. 2010) in the horizontal plane at 45% (**a**) and 57% (**b**) from the dorsal top point in the dorsoventral extent of the whole cerebellum and in the longitudinal plane at 80% (**c**), 68% (**d**), 57% (**e**), 45% (**f**) and 34% (**g**) from the midsagittal plane to the lateral pole of the AA in the mediolateral extent of the cerebellum. Each

marmoset cerebellar section is compared with a drawing of macaque cerebellar section of 7.0-Tesla MR imaging at an equivalent level (horizontal sections at 42 and 63% in the dorsoventral extent of the whole cerebellum; sagittal sections at 83, 71, 59, 47 and 35% in the mediolateral extent from the midsagittal section to the lateral pole of the AA). **h** MR images of macaque cerebellum for panels **a**, **b** and **f**. Refer to Table 1 for correspondence between nomenclatures in this figure and in previous studies. Scale bars 1 mm (**a** top, **b** top, **c–g** left), 5 mm (**a** bottom **b** bottom, **c–g** bottom, **h**). II–IX lobule II–IX, AA ansiform area, B sublobule B, C caudal, D dorsal, FI flocculus, H hemispheric, Lt left, PFI paraflocculus, R rostral, Rt right, V ventral

(Kelly and Strick 2003; Strick et al. 2009; Sugihara et al. 2009; Fujita et al. 2010; Steele et al. 2016). Projection patterns that help highlight lobule identification in the crus I/II area are reviewed below.

### Climbing fiber axons

In rat, the basic projection pattern of climbing fiber axons at the single axon morphological level demonstrates a topographic relationship to the longitudinally striped structure of the cerebellum and to their lobular organization (Voogd et al. 2003; Sugihara and Shinoda 2004, 2007; Pijpers et al. 2006; Fujita and Sugihara 2013). Therefore, we hypothesized that homologous lobules are expected to have similar axonal projection patterns among different animals.

To test the topographic relationship between the longitudinally-stripped structure and the trajectory of single axon morphologies, we analyzed the axons terminating in the longitudinal stripes of zone C2 (aldolase C stripe 4+//5+, axons in Fig. 6b, c), zone C3 (aldolase C stripe 4-//5-, axon in Fig. 6d) and zone D2 (aldolase C stripe 6+//7+, axons in Fig. 6a), ranging from the paravermis to the hemisphere (indicated in Fig. 6; c.f. Voogd et al. 2003; Sugihara and Shinoda, 2004 for definitions of zones and aldolase C stripes), in simple lobule (HVI), crus I (AA), and crus II and paramedian lobule (HVIIB) in rat. The distribution of climbing fiber axonal branching (Sugihara et al. 2001; Fujita and Sugihara 2013) was analyzed in relation to the lobular organization (Fig. 6a–d). Based on the climbing fibers' target lobules, axons were classified into two groups: (1) simple lobule (HVI) and/or crus II/paramedian lobule (HVIIB)-projecting axons which often projected to both simple lobule and crus II/paramedian lobules (Fig. 6c, d), and (2) crus I (AA)-projecting axons, which projected only to crus I or were sometimes accompanied by branching into the paraflocculus (Fig. 6a, b). No axons projected to both crus I and simple lobule, or to both crus I and crus II/paramedian lobule in our olivocerebellar axonal reconstructions in the paravermis or hemisphere in the rat cerebellum ( $n = 6$  axons shown in Figs. 4 and 6a–d other axons).

To determine whether a similar lobular distinction pattern exists in the olivocerebellar projection in the marmoset cerebellum, we examined the marmoset olivocerebellar projection from the data of our previous study (Fujita et al. 2010). A large injection of BDA into the HVIIB (crus II—Larsell/Brodal definition, in Fujita et al. 2010) labeled climbing fibers retrogradely in lobules V and HVI primarily in zone C3 and D1 (aldolase C stripes 4-//5- and 5+//6+, Fig. 6f). Labeled climbing fibers were mapped on a sample parasagittal section of the marmoset cerebellum (Fig. 6e). The mapping revealed that almost all labeled

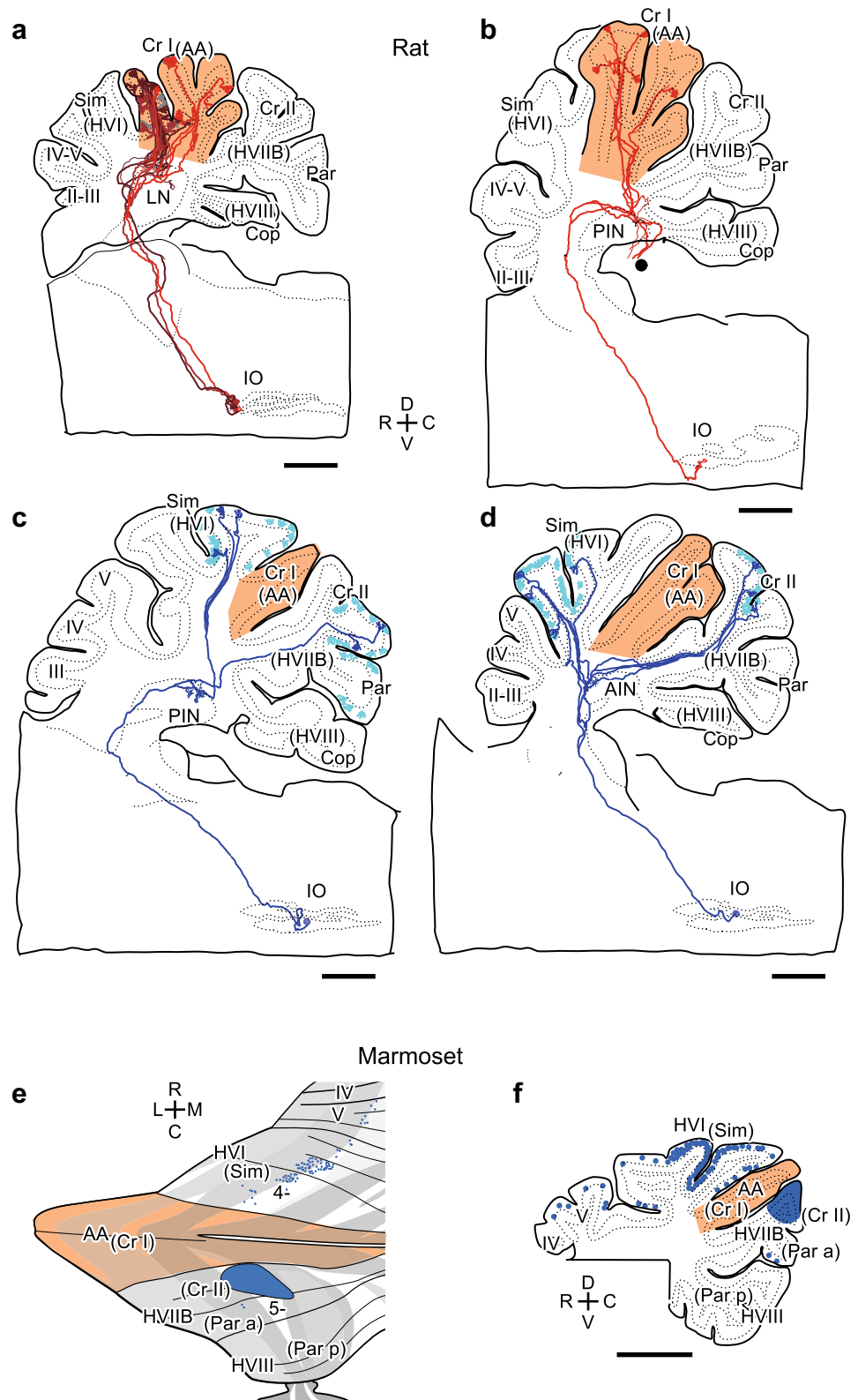
climbing fibers were located in lobule HVI (simple lobule) with only a few labeled climbing fibers located in lobule HVIIB outside the injection site. However, no climbing fibers were labeled in the AA (crus I—Larsell/Brodal definition, in Fujita et al. 2010). This indicated that in marmoset the population of inferior olive neurons projecting to the AA was distinct from the population of inferior olive neurons projecting to HVI and/or HVIIB. The pattern of lobule dependency in the olivocerebellar axonal projection in marmoset was the same as that in rat (Fig. 6c, d), thereby supporting homology of the AA between rat and marmoset.

### Purkinje cell axons

In our previous work, projections of four individual Purkinje cell axons (Sugihara et al. 2009) originating from crus I (AA) and crus II (HVIIB) were reconstructed in rat. Here, we reconstructed six additional Purkinje cell axons originating from these lobules. Since all ten axons belonged to zone C2 (aldolase C stripe 4+//5+ in the paravermis, Groenewegen et al. 1979; Sugihara et al. 2009) and terminated in the posterior interposed nucleus (PIN), the correlation between the target area within the PIN and the lobule of origin was examined. All the four axons that originated from crus II (HVIIB) terminated in the rostradorsal part of the PIN (Fig. 7a, red axon). Five out of the six axons originating from crus I (AA) terminated in the central to caudoventral part of the PIN (Fig. 7a, blue axon). Only one out of the six axons originating from the rostral end of the most rostral folia of crus Ia (AA), near the bottom of the fissure between simple lobule (HVI) and crus I, terminated in the dorsal and central part of the PIN (the case shown in Fig. 7a of Sugihara et al. 2009). This result indicated a difference in the projection pattern of Purkinje cell axons originating in crus I (AA) and crus II (HVIIB), even though they all belonged to the same longitudinal stripe (zone C2). Since the location of the injection site for a single case was near the simple lobule (HVI), we have reason to believe that in this exceptional case, the Purkinje cell in crus Ia that terminated in the dorsal PIN may represent the projection pattern of Purkinje cells in simple lobule (HVI). In a previous retrograde labeling study, the dorsal part of the lateral nucleus was innervated by Purkinje cells from zone D2 (aldolase C stripe 6+//7+) in simple lobule (HVI) and crus II/paramedian lobule (HVIIB) in the rat (Sugihara et al. 2009), suggesting that the ventrodorsal target separation of Purkinje cell projections from crus I (AA) and neighboring lobules are not unique to zone C2, but also present in other neighboring zones.

In marmoset, data from our previous study allowed us to map the target area of fluorescently labeled Purkinje cells

**Fig. 6** Distinct projection of olivocerebellar climbing fiber axons in the AA (crus I in rat) and adjacent lobules in rat (**a–d**) and marmoset (**e, f**). **a** Three reconstructed axons, all of which terminate only in crus I (AA). Redrawn from Fig. 4 of Sugihara et al. (2001). **b** One axon terminating in crus I (AA) and in the paraflocculus (filled circle, not included in the figure). Redrawn from Fig. 1a of Fujita and Sugihara (2013). **c, d** Axons terminating in simple lobule (HVI) and crus II (HVIIB) but not in crus I (AA). Redrawn from Fig. 2b, c of Sugihara et al. (2001). Labeled climbing fibers that did not belong to the reconstructed axon are shown in light blue. **e, f** Climbing fiber terminals labeled with BDA injected in HVIIB (crus II). All climbing fiber terminals were flattened in a sample sagittal section (**f**) and plotted on the unfolded scheme (**e**). Re-analysis of data obtained in Fujita et al. (2010). **f** is a redrawing of one case in Fig. 7 of Fujita et al. (2010). Lobule names in parenthesis are under Larsell/Brodal definition in **e** and **f**. ‘4-’ and ‘5-’ are names of aldolase C stripes in **e**. Scale bars 1 mm (**a–d**), 2 mm (**f**). II–VIII lobule II–VIII, *a, B, p* sublobule a, B, p, AA ansiform area, AIN anterior interposed nucleus, C caudal, Cop copula pyramidis, Cr I crus I, Cr II crus II, D dorsal, H hemispheric, IO inferior olive, L lateral, LN lateral nucleus, M medial, Par paramedian lobule, PFI paraflocculus, PIN posterior interposed nucleus, R rostral, right, Sim, simple lobule, V ventral



(Fujita et al. 2010). We reanalyzed two cases in which the injection of fluorescently tagged dextran was located in zone C2 (or aldolase C stripe 4+/5+) in the AA (crus I—

Larsell/Brodal definition,  $n = 1$ ) and HVIIB (crus II—Larsell/Brodal definition,  $n = 1$ ). In these samples, the termination regions of Purkinje cell axons originating from

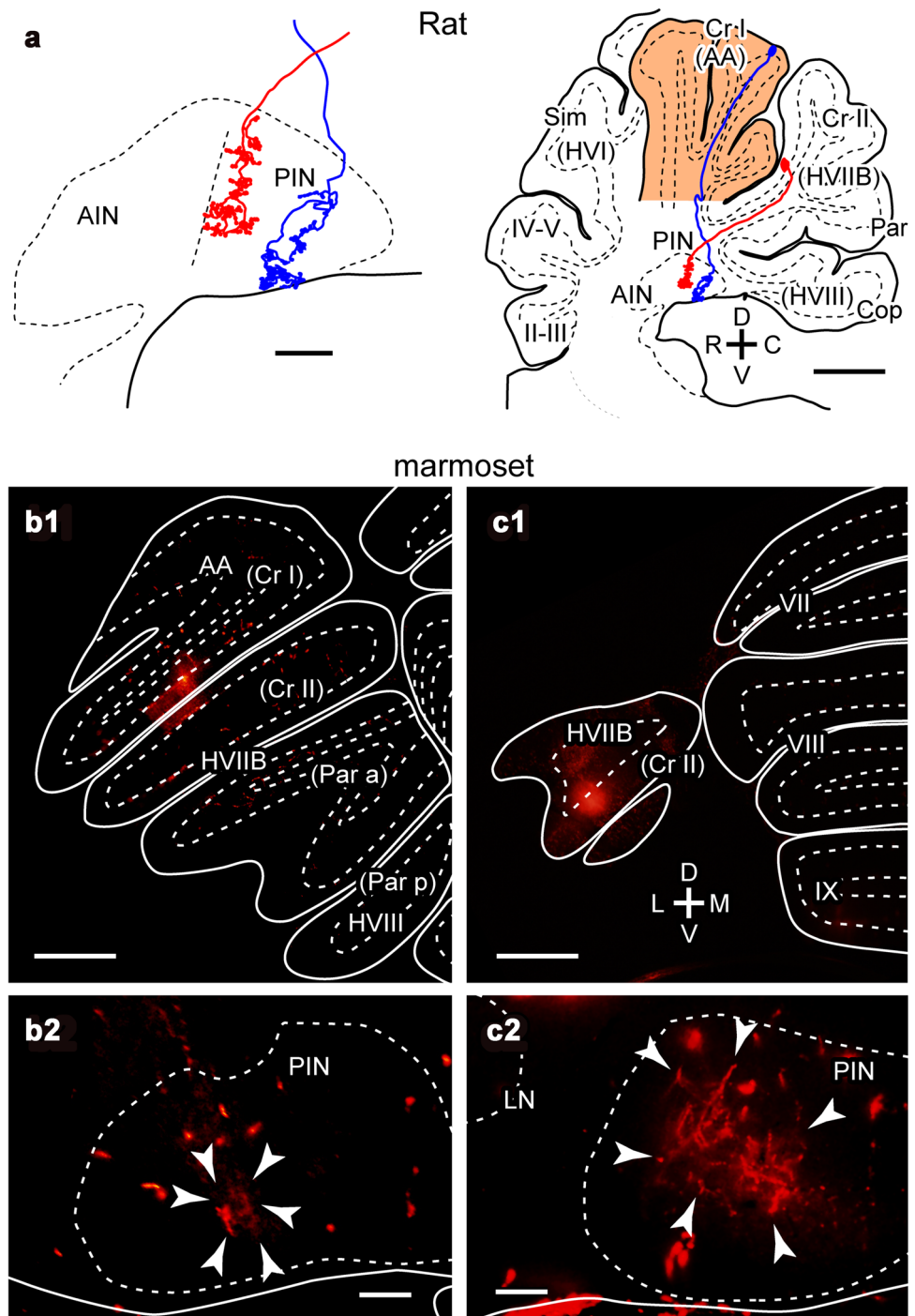


**Fig. 7** Projection patterns of Purkinje cell axons from the AA (crus I in rat) and HVIIB (crus II in rat) to the posterior interposed nucleus (PIN).

**a** Reconstruction of two BDA-labeled rat Purkinje cell axons originating from aldolase C stripe 4+//5+ (module C2) and terminating in the PIN. The axon that originated in crus I (AA) terminated in the ventrocaudal PIN (*blue*), while the axon that originated in crus II (HVIIB) terminated in the dorsostral PIN (*red*, each axon is from different individuals).

**b, c** Two cases of fluorescent dextran labeling of Purkinje cell axons in marmoset. Injection site in the AA (**b1, c1**) and labeled Purkinje cell axon terminals in the PIN (**b2, c2**). The section in **c2** is located more rostrally than the section in **b2** as noted by the presence of the lateral nucleus.

Arrowheads indicate labeled axonal terminals to distinguish artifact labeling of blood vessels. Data in **b** and **c** were obtained from our previous study (Fujita et al. 2010) but newly arranged for this figure. Scale bars 200  $\mu$ m (**a left**), 1 mm (**a right**), 1 mm (**b1, c1**), 200  $\mu$ m (**b2, c2**). II–VIII lobule II–VIII, *a, B, p* sublobule *a, B, p*, AA ansiform area, AIN anterior interposed nucleus, C caudal, Cop copula pyramidis, *Cr I* crus I, *Cr II* crus II, D dorsal, H hemispheric, L lateral, LN lateral nucleus, M medial, Par paramedian lobule, PIN posterior interposed nucleus, R rostral, right, Sim simple lobule, V ventral



the AA were located more caudally and ventrally in the PIN (Fig. 7b1, 2) than those of axons originating from the HVIIB (Fig. 7c1, 2). This positional relationship of Purkinje cell termination in the PIN was similar to that in rats (Fig. 7a). This supports the notion that the lobules designated as AA are homologous in rats and marmosets. In addition, Purkinje cells in zone D2 (or aldolase C stripe 6+//7+) in HVIIB do not project to the ventral part but to the centrolateral part of the lateral nucleus (case 'n' in

Fig. 7 of Fujita et al. 2010), conforming to the notion above. Thus, the Purkinje cell output pathways originating from the AA and neighboring lobules (HVI and HVIIB) are separated into ventral and dorsal areas, respectively, within the PIN in both rat and marmoset. Furthermore, this separation may also occur in the lateral (dentate) nucleus in rats and marmosets.

In a viral tracing study in capuchin monkey, the AA (crus I/II—Paxinos definition) and neighboring lobules



(HVI and HVIIB) project to the ventral and dorsal part of the dentate nucleus, respectively (Kelly and Strick 2003; Strick et al. 2009). Tractography analysis in human cerebellum demonstrated that Purkinje cells in the AA (crus I/II) project to the ventral part of the dentate nucleus, while HIV, HV and HVI-originating Purkinje cells project to the dorsal part of the dentate nucleus (Steele et al. 2016).

By defining the AA as proposed in this article, the topography of Purkinje cell projections from crus I/II to the PIN and the lateral nucleus (dentate nucleus) can be understood consistently in rodents, non-human primate and human. The AA projects ventrally, while neighboring lobules project dorsally.

### Pontine mossy fiber axons

The basilar pontine nucleus (BPN) is the main source of mossy fiber afferents to the AA (Brodal 1981). In macaque, retrograde tracing from the AA (crus I—Larsell/Brodal definition) labeled precerebellar neurons in the rostromedial pons, whereas retrograde tracing from neighboring lobules (HVI, HVIIB and HVIII) labeled neurons in the more central areas (Brodal 1979; Brodal and Bjaalie 1992). The rostromedial part of the macaque BPN receives input from the prefrontal cortex, whereas the central area of the basilar pontine nucleus receives inputs from the motor and somatosensory cortices (Glickstein et al. 1985; Huerta et al. 1986; Shook et al. 1990; Schmahmann and Pandya 1997).

In rodents, crus I (AA) receives projections mostly from rostral and peripheral (medial or lateral) areas of the BPN, whereas the simple lobule (HVI), crus II and paramedian lobule (HVIIB) receive projections mostly from central areas (Fig. 3 of Burne et al. 1978; Figs. 4–7 of Mihailoff et al. 1981). Thus, the topography of the pontocerebellar projection supports our identification of the AA in primates and rodents.

### Comparative molecular expression patterns between mouse and marmoset

The longitudinally stripe-shaped pattern of aldolase C (zebrin II) expression in Purkinje cell subsets has been originally reported in rat (Hawkes and Leclerc 1987), but found to be conserved in other mammals including primates (Sillitoe et al. 2005). The stripe-shaped pattern is highly variable across lobules but well conserved among individuals (Hawkes and Leclerc 1987; Fujita et al. 2014). Therefore, we hypothesized that lobule-dependent aldolase C expression pattern between animals should help identify homologous cerebellar lobules. The aldolase C expression pattern in the hemisphere of rats and mice

demonstrated that crus I (AA) is mostly aldolase C-positive, while neighboring lobules (simple lobule or HVI, which is rostral to crus I, and crus II/paramedian lobule or HVIIB, which is caudal to crus I) had alternating positive and negative stripes (Fujita et al. 2014; Fig. 8a, dark and light colors indicate positive and negative areas, respectively). In the marmoset cerebellum, we made a three-dimensional (3D) reconstruction of the Purkinje cell layer in which the intensity of aldolase C expression is depicted in gray (Fujita et al. 2010). We rotated the 3D model in order for the surface of the AA (crus I—Larsell/Brodal definition) to be viewed in the center of the field of view (Fig. 8b). This method revealed that the AA was mostly aldolase C-positive as shown by dark grayish color covering the majority of the AA (Fig. 8b). The area in blue indicates the gap in the cortical structure where the white matter is exposed on the surface of the cerebellum (Fujita et al. 2010). Such a gap was also present in the rat AA but not in the apex region (next section). Interestingly, the neighboring lobules (HVI and HVIIB) had alternating positive and negative stripes (Fig. 8b). These results indicate that the AA, as defined in this study, is homologous between the mouse and marmoset. The schematic representation of aldolase C stripes in the unfolded cerebellar cortex of the mouse (Fujita et al. 2014) and marmoset (Fujita et al. 2010) supports this conclusion (Fig. 8c, d).

Expression of aldolase C is linked with expression of other molecules. Phospholipase C beta3 (Plcb3) is widely expressed throughout most of crus I (AA) but expressed in alternating stripes in other lobules, similar to aldolase C, in rat (Sarna et al. 2006). On the contrary, Plcb4 is expressed in a complementary pattern: scarcely expressed in crus I (AA) in rodents (Sarna et al. 2006). Developmentally, clusters of Purkinje cell subsets in crus I (AA) are generally distinct from clusters in neighboring lobules in the mouse (Fujita et al. 2012). While clusters in crus I (AA) often express INM13 and protocadherin 10 (Pcdh10), clusters in neighboring lobules often express Plcb4 and Epha4 (Fujita et al. 2012). Therefore, molecular expression patterns in crus I (AA) are different from those of neighboring lobules. We argue that these organizational patterns are related to the formation of adult neuronal connections underlying specific functions of the AA.

### The gap in the cortical structure as a possible landmark for the ansiform area

The outer surface of the cerebellum is generally covered with a continuous sheet of the cortical structure except for lateral edges of cerebellar lobules. However, this continuous sheet is disrupted by a small gap in a few particular

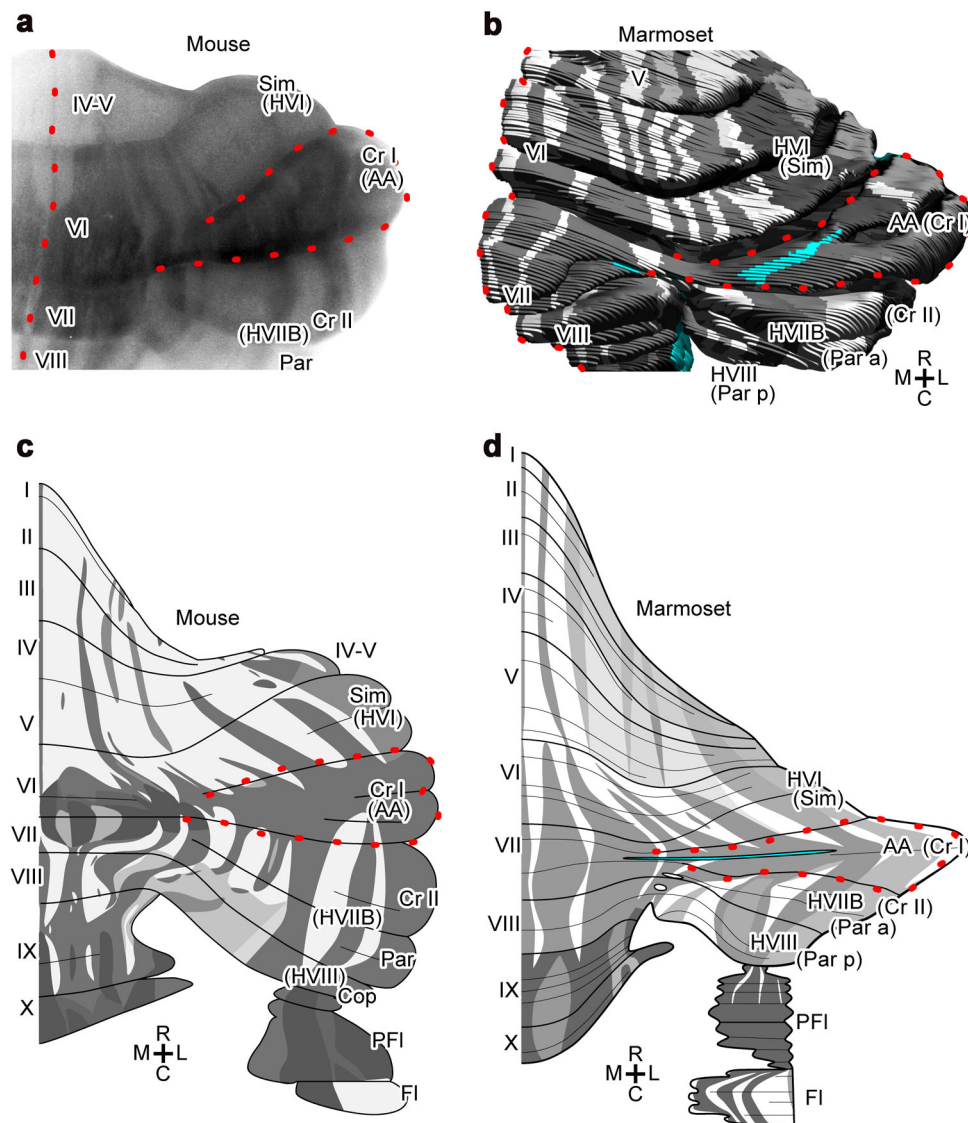


**Fig. 8** Aldolase C (zebrin II) expression pattern in the cerebellar cortex to aid in identifying homologous lobules between mouse and marmoset. **a** Color-inverted epi-fluorescent photography of a whole cerebellum preparation from an Aldoc-Venus mouse (Fujita et al. 2014). **b** Three-dimensional reconstruction of the Purkinje cell layer in the marmoset cerebellum (Fujita et al. 2010) viewed from the dorso-caudo-lateral direction, to center the AA in the field of view. Blue area indicates a gap of the cortical layers in the AA (Fujita et al. 2010). **c** Drawing of aldolase C stripes in the entire cerebellar cortex of mouse (right side, reproduced from Fujita et al. 2014). **d** Drawing of aldolase C stripes in the entire cerebellar cortex of marmoset (right

side). **d** was redrawn from Fig. 6 of Fujita et al. (2010). In all panels, dark (gray) and light (white) colors indicate positive and negative areas, respectively. Proposed consistent nomenclature is shown in parenthesis for rat (**a**, **c**), while the nomenclature in the original articles (Larsell/Brodal definition) is shown in parenthesis for marmoset (**b**, **d**). Red dashed curves outline the AA (crus I in rat) and indicate the midline (in **a–d**). I–X lobule I–X, a, B, p sublobule a, B, p, C caudal, AA ansiform area, Cop copula pyramidis, Cr I crus I, Cr II crus II, FI flocculus, H hemispheric, L lateral, LN lateral nucleus, M medial, Par paramedian lobule, PFI paraflocculus, PIN posterior interposed nucleus, R rostral, right, Sim simple lobule

caudal surface of lobule VIc (rat, Fig. 2 of Sugihara and Shinoda 2004; marmoset: Fujita et al. 2010). In these areas, the white matter or the granular layer is exposed to the cerebellar surface since the entire cortical structure or the molecular and Purkinje cell layers are missing. Gaps are found in two separate areas in the rat and marmoset cerebellum similarly; one in the paravermal region of the

caudal surface of lobule VIc (rat, Fig. 2 of Sugihara and Shinoda 2004) or VIIAc (marmoset, filled arrowheads in Fig. 4 of Fujita et al. 2010), which are equivalent lobules in spite of their different names (Fujita et al. 2010), and the other at the vermis-hemisphere (or vermis-paravermis) boundary in lobule VII under the paravermal vein (rat: Fig. 2 of Sugihara and Shinoda 2004; marmoset: open

arrowheads in Fig. 4 of Fujita et al. 2010). The gap reported in the mouse cerebellum (Figs. 1–1, 2–1 of Marani and Voogd 1979) is located in the latter position at the vermis–paravermis boundary in lobule VII.

We re-examined the location of the former gap in the rat, mouse and marmoset cerebellums. We confirmed that its medial end was allocated in the paravermal region from which the AA (crus I in rat and crus I or crus I–II in marmoset, depending on nomenclature) expanded laterally in both species (Fig. 9b, c, e). While this gap was small in the rat, it was elongated laterally for a certain distance toward the center of the AA in the marmoset (Fig. 8b, blue transverse band). A gap is present in the paravermal AA in the macaque cerebellum (Fig. 9a, d; sagittal and horizontal sections: Figs. 23–38 and 47–48, respectively, in Madigan and Carpenter (1971); coronal sections: Plate 138 and 139 in Paxinos et al. 2009). A gap is also present in the paravermal AA in the mouse cerebellum (Fig. 9f). Thus, we propose that the position of the gap in the paravermal AA is conserved among mammals.

## Evolutionary and functional distinctions of the mammalian cerebellar ansiform area

The difference in relative size of the AA (or crus I/II under the Paxinos-type definition) has been correlated with different evolutionary non-motor traits among primate species (Balsters et al. 2010; Smaers 2014). We hypothesize that the involvement of the AA in non-motor functions may be applicable to other mammalian species including rodents.

The AA shows a significant increase in volume fraction in the whole cerebellum in more skillful species including human (36.6%), chimpanzee (29.5%) and capuchin monkey (20.5%) (crus I/II—Paxinos-type definition, Balsters et al. 2010). Our measurement of volume fraction of the human AA within the whole cerebellar volume resulted in a similar value (34.2%) to that of Balsters et al. (2010). Our measurements in the macaque and marmoset expanded the range of the AA volume fraction increase in relation to the skillfulness in primates by up to 9.2% (marmoset)—34.2% (human) (Fig. 10).

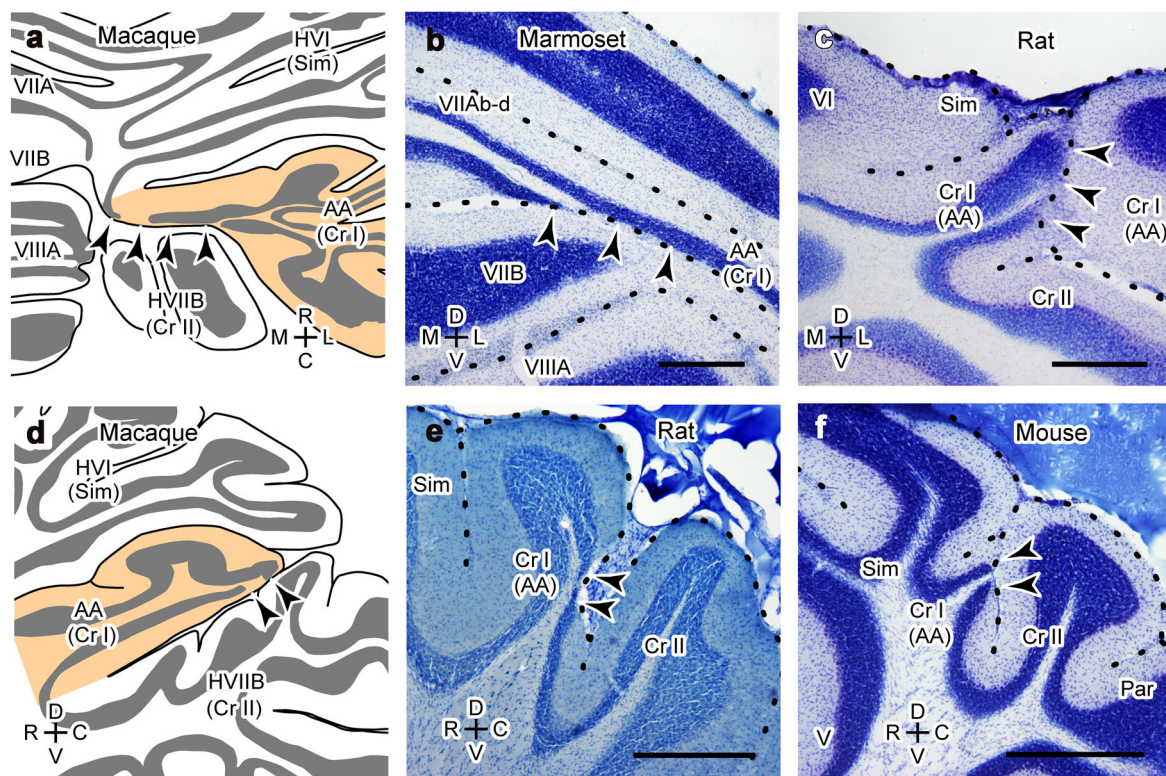


**Fig. 9** Gap in the cortical structure located in the paravermal area of the AA in photomicrographs or drawings of sections of the primate and rodent cerebellum. **a** *Horizontal* section of the macaque cerebellum. Drawing was reproduced from Fig. 48 of Madigan and Carpenter (1971). **b** *Coronal* section of the marmoset cerebellum. **c** *Coronal* section of the LE rat cerebellum. **d** *Sagittal* section of the macaque cerebellum. Drawing was reproduced from Fig. 32 of Madigan and Carpenter (1971). **e** *Sagittal* section of the Wistar rat

cerebellum. **f** *Sagittal* section of the ICR mouse cerebellum. *Arrowheads* indicate the gap in the medial part of the AA in all panels. The nomenclature in the original articles (Larsell/Brodal definition) is shown in *parenthesis* for macaque (**a, d**). *Scale bars* 500  $\mu\text{m}$  (**b, c, e and f**). *V–VII* lobule V–VII, *A, B, a, d, p* sublobule A, B, a, d, p, *AA* ansiform area, *C* caudal, *Cr I* crus I, *Cr II* crus II, *D* dorsal, *H* hemispheric, *L* lateral, *M* medial, *R* rostral, *Par* paramedian lobule, *Sim* simple lobule, *V* ventral



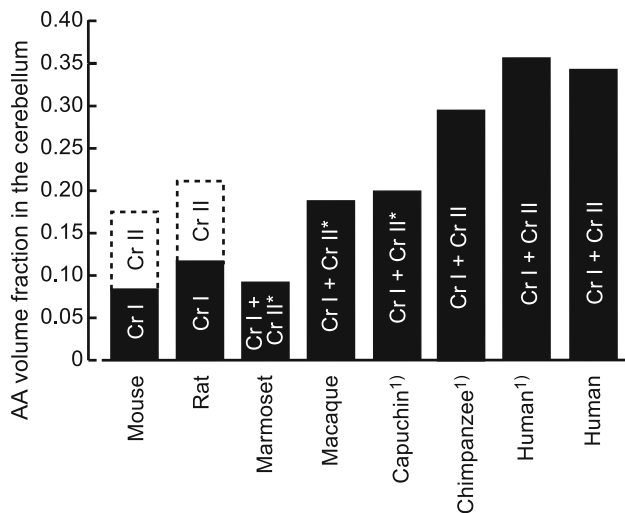


**Fig. 10** Volume fraction of the AA in the whole cerebellum in various species of the Euarchothogliares clade. Volume fraction of the AA (crus I/II in human; crus I/II—Paxinos type definition in macaque and marmoset; crus I in rat and mouse) and crus II (rat and mouse) was the average of the measurements in horizontal and sagittal sections in one or two brain sample(s) (see “Materials and methods”). Volume fraction of the AA (crus I/II in human<sup>1)</sup>, chimpanzee<sup>1)</sup> and capuchin<sup>1)</sup> was also obtained from Table 1 of Balsters et al. (2010) by dividing the sum of the volumes for crus I and crus II over the whole cerebellum volume (average of ten cases in MR imaging in living samples). Asterisk indicates the Paxinos-type definition in non-human primates. *Cr I* crus I, *Cr II* crus II

The volume fraction of crus I and crus II in the whole rat and mouse cerebellum demonstrated that the total volume fraction of crus I plus crus II in rodents (black plus white bar in rat and mouse columns in Fig. 10) is much larger than the volume fraction of the AA (crus I/II—Paxinos-type definition) in the marmoset. This is difficult to interpret if we assume crus I/II (or the AA) expands in relation to the dexterity of mammals. Thus, the volume fraction of crus I and crus II in rodents supports our identification of the AA (AA = crus I in rodents, AA = crus I/II—Paxinos-type definition in primates). The volume fraction of the AA in rat (11.7%) and mouse (8.4%) is of similar range to that of marmoset (9.2%).

In terms of function, human imaging studies suggest that crus I/II (AA) is primarily involved in non-motor, cognitive, language and saccadic functions (Stoodley and Schmahmann 2009; Batson et al. 2015), which is different from its neighboring lobules involved in sensorimotor tasks. Non-human primate studies characterize crus I/II—Paxinos definition (AA) by their connectivity to the prefrontal and parietal cortex through the ventral part of the dentate nucleus underlying non-motor functions (Strick et al. 2009; Fig. 13 of Glickstein et al. 2011). Although crus I and crus II have been grouped as two individual parts comprising the AA in human and non-human

primate under Paxinos’ definition in this study, it is to be noted that there are functional and connectivity differences between crus I and crus II (rostral and caudal parts of the AA) in human and non-human primates (Buckner et al. 2011). In rodents, only a few studies compared functional localizations in crus I and crus II (Shambes et al. 1978; Welker 1987). Mapping of mossy fiber activity in rats has shown that while crus I receives ipsilateral projections from receptive fields on the dorso-lateral regions of the head and upper face, crus II is responsive to perioral, lip, incisors and intraoral skin bilaterally, and the paramedian lobule receives input from the entire body surface, perioral area, head, forelimbs, trunk and hindlimbs bilaterally (Shambes et al. 1978). While the receptive fields of crus I are ipsilateral, receptive fields of crus II and paramedian lobule are ipsilateral (in the lateral area of the lobules), bilateral (in the intermediate area) and contralateral (in the medial area). This suggests some functional separation between crus I and crus II-paramedian lobule. Moreover, the simple lobule, which is rostral to crus I, receives input from bilateral perioral and intraoral skin, similar to crus II (Welker 1987). Based on these studies, the rodent crus II has been used in many physiological and anatomical inquiries in combination with somatosensory stimulation to the vibrissa of facial area mediated by climbing or mossy fibers (Llinás and Sasaki 1989; Hartmann and Bower 2001; Hanson et al. 2000). Although some reports describe that somatosensory response which is mainly observed in crus II is extended into crus I, response is generally clearer in crus II compared to crus I (Figs. 3, 4 of Hanson et al. 2000). Lesions in crus I (AA), simple lobule (HVI) and hemispheric lobule V produce impairment of visually guided forelimb movement in the rat (Aoki et al. 2013), although the specific lobule responsible for this remains to be determined. Anatomical evidence for functional separation of the rat crus I and II is partially inferred by transsynaptic connection between crus II and the somatosensory, motor and premotor cortices as revealed with a rabies viral vector (Suzuki et al. 2012), which conforms to the motor function of these lobules. This study, however, did not examine projection to crus I.

Due to the similarity in axonal projections between the rat and primate AA, we argue that the rodent AA has a specific role related to non-motor functions reported in the primate AA, though this possibility remains to be tested in future studies. If the rodent AA can be a model region to study the evolutionary basis of cerebellar non-motor function, the greater availability of genetic approaches and a broader range of experimental procedures in rodents render rodent models beneficial to studying aspects of non-motor function in the cerebellum.



## Functional and anatomical consistencies and inconsistencies in other cerebellar lobules among primates and rodents

Besides the function of crus I and crus II, cerebellar function is not consistently understood in the paraflocculus and vermal lobule VII between primates and rodents. The paraflocculus, the ventral part in particular, is involved in control of smooth pursuit voluntary eye movements in primates (Shidara and Kawano 1993). However, the function of the paraflocculus has not been studied much in rodents except in relation to tinnitus (Bauer et al. 2013). There seem no inconsistencies in the anatomical identification of the paraflocculus lobule between primates and rodents.

Relative to other vermal lobules, lobules VI–VII (or lobules V–VIII) have a stronger connection with the cerebral cortex than with the spinal cord or the vestibular system (Glickstein et al. 2011; Coffman et al. 2011). In primates, lobule VII is connected with the frontal eye field of the cerebral cortex and is mainly involved in control of voluntary eye movements such as saccades (Catz and Their 2007). Lobule VII's output nucleus, the caudal fastigial nucleus, affects wide areas in the frontal, insular, parietal and occipital cortices (Sultan et al. 2012). In human, vermal lobule VII, as well as crus I/II, is involved in non-motor function (Stoodley and Schmahmann 2009; Batson et al. 2015).

Concerning anatomical consistency of lobule VII between primates and rodents, we have proposed that lobules VIb, VIc and VII in rodents are homologous to lobule VII in primates, whereas lobule VIa in rodents is homologous to lobule VI in primates, based on foliation pattern, aldolase C striped pattern and position of the Purkinje cell gap (Fujita et al. 2010). Similar to vermal lobule VII in primates, vermal lobules VIb–c and VII in rodents do not receive spinal cord or cuneate inputs (Quy et al. 2011). Rat vermal lobules VI–VII are innervated by medial and lateral areas of the BPN (Graybiel 1974), similar to crus I (Burne et al. 1978; Mihailoff et al. 1981). Viral vector tracing showed axonal connection between vermal lobules VI–VII and the prefrontal cortex in rat, suggesting their involvement in non-motor function (Suzuki et al. 2012; Watson et al. 2014). Therefore, besides the AA, vermal lobules VI–VII may also be a possible target area for studying neuronal mechanisms underlying non-motor or visuomotor functions of the cerebellum in rodents.

## Concluding remarks

This article demonstrated evidence for currently existing inconsistencies in the nomenclature of crus I and crus II in rodents, non-human primates and humans. Simple

morphological examination of the cerebellar surface and tissue sections provided in this article enabled the identification of homologous lobules between human, non-human primate, and rodent cerebellum, confirming an inconsistency in nomenclature in the literature. Using the marmoset cerebellum, comparison between primate and rodent lobulation was facilitated because the less foliated marmoset cerebellum revealed the basic foliation plan and resolved the discrepancy between the nomenclatures. We concluded that the following lobules were homologous: (1) crus I in rodents, (2) crus I in non-human primates under the Larsell/Brodal definition, (3) crus I/II in human, and (4) crus I/II in non-human primates under the Paxinos definition. Therefore, we referred to these homologous regions as the AA. The topographic axonal projections and aldolase C molecular expression patterns underpin the inter-species homology of these lobules. The morphological, functional and evolutionary aspects of the mammalian crus I/II areas of the cerebellar hemisphere would be better understood and studied under the new definition of homologous lobules provided in this article. Although this article is focused on the cerebellum of rodents and primates, the idea behind the proposed AA is applicable to other mammalian species. However, the identification of homologous lobules may require further analysis in other areas of the mammalian cerebellum. For example, homology of the ansula lobule, which has been defined around the boundary between crus II and paramedian lobule in the bear and cat cerebellum (Bolk 1906; Groenewegen et al. 1979), remains unclear in the cerebellum of other mammals. The hemispheric part of lobule VIII (or pyramis, Smith 1902) has been named copula pyramidis (Smith 1902) since it is continuous to the paraflocculus in the rodent cerebellum (Larsell 1952), but it has been defined as a part of the paramedian lobules in the monkey and cat cerebellum (Larsell 1953). The paraflocculus also has a substantial difference in organization among primates, cat, rabbit and rodents (cf. Voogd and Barmack 2006).

**Acknowledgements** The authors thank Dr. Jan Voogd for his valuable comments to the manuscript, as well as, Dr. Enrico Marani for sending us a critical reference on mouse cerebellar morphology, Drs. Takafumi Minamimoto (NIRS) and Arata Oh-Nishi (NIRS) for providing the macaque (Japanese monkey) specimen, Dr. A. O.-N. for discussion, Nobuhiro Nitta (NIRS) for technical assistance in the MR imaging experiments, Prof. Emi Schinzingler for interpreting German literature, Gideon Anokye Sarpong for reading the manuscript, and Mr. Minoru Takada for technical assistance. This study was supported by Grant-in-Aid for Scientific Research from the Japan Society for the Promotion of Science (KAKENHI; to I.S., 16K070025, 26•04381; to H.F., 26430035; to I.A., 24300167) and COI STREAM Grant of the Ministry of Education, Culture, Sports, Science and Technology (MEXT) of Japan (to I.A.). Y.L. was a recipient of the TMDU self-financing international student special research grant and is a recipient of the MEXT scholarship. H.F. was supported by the JSPS postdoctoral fellowship for research abroad. M.S.B. is a recipient of the

MEXT scholarship. S.Y. is a recipient of the JSPS invitation fellowship for Research in Japan (Short-Term). H.N. is a recipient of the JSPS Postdoctoral Fellowship for Overseas Researchers.

**Authorship contributions** All authors listed had full access to all the data in the study and take responsibility for the integrity of the data and the accuracy of the data analysis. Study concept and design: HF, IS. Acquisition of data: YL, IS (human, macaque, marmoset, rat, mouse), HF (marmoset, rat, mouse), MSB, SY (human), CS, MT, IA (human, macaque). Analysis and annotation of data: YL, HF, IS. Drafting of the manuscript: YL, HF, HN, SY, IS. Critical revision of the manuscript for important intellectual content: HF, HN, IS. Statistical analysis: YL, IS. Obtained funding: HF, IA, IS. Administrative, technical, and material support: KA, TH, IA, IS. Study supervision: IS.

#### Compliance with ethical standards

**Conflict of interests** The authors declare no competing financial interests.

## References

- Aoki S, Sato Y, Yanagihara D (2013) Lesion in the lateral cerebellum specifically produces overshooting of the toe trajectory in leading forelimb during obstacle avoidance in the rat. *J Neurophysiol* 110:1511–1524. doi:[10.1152/jn.01048.2012](https://doi.org/10.1152/jn.01048.2012)
- Balsters JH, Cussans E, Diedrichsen J, Phillips KA, Preuss TM, Rilling JK, Ramnani N (2010) Evolution of the cerebellar cortex: the selective expansion of prefrontal-projecting cerebellar lobules. *Neuroimage* 49:2045–2052. doi:[10.1016/j.neuroimage.2009.10.045](https://doi.org/10.1016/j.neuroimage.2009.10.045)
- Barmack NH, Baughman RW, Eckenstein FP, Shojaku H (1992) Secondary vestibular cholinergic projection to the cerebellum of rabbit and rat as revealed by choline acetyltransferase immunohistochemistry, retrograde and orthograde tracers. *J Comp Neurol* 317:250–270
- Batson MA, Petridou N, Klomp DWJ, Frens MA, Neggers SFW (2015) Single session imaging of cerebellum at 7 tesla: obtaining structure and function of multiple motor subsystems in individual subjects. *PLoS One* 10:e0134933. doi:[10.1371/journal.pone.0134933](https://doi.org/10.1371/journal.pone.0134933)
- Bauer CA, Kurt W, Sybert LT, Brozoski TJ (2013) The cerebellum as a novel tinnitus generator. *Hear Res* 295:130–139
- Bolk L (1906) *Das Cerebellum der Säugetiere, Eine Vergleichend Anatomische Untersuchung*. Verlag von Gustav Fischer, Jena
- Brodal P (1979) The pontocerebellar projection in the rhesus monkey: an experimental study with retrograde axonal transport of horseradish peroxidase. *Neuroscience* 4:193–208
- Brodal A (1981) *Neurological anatomy in relation to clinical medicine*, 3rd edn. Oxford University Press, New York
- Brodal P, Bjaalie JG (1992) Organization of the pontine nuclei. *Neurosci Res* 13:83–118
- Buckner RL, Krienen FM, Castellanos A, Diaz JC, Yeo BTT (2011) The organization of the human cerebellum estimated by intrinsic functional connectivity. *J Neurophysiol* 106:2322–2345. doi:[10.1152/jn.00339.2011](https://doi.org/10.1152/jn.00339.2011)
- Buisseret-Delmas C (1988) Sagittal organization of the olivocerebellonuclear pathway in the rat. II. Connections with the nucleus interpositus. *Neurosci Res* 5:494–512
- Buisseret-Delmas C, Angaut P (1989) Sagittal organisation of the olivocerebellonuclear pathway in the rat. III. Connections with the nucleus dentatus. *Neurosci Res* 7:131–143
- Burne RA, Eriksson MA, Saint-Cyr JA, Woodward DJ (1978) The organization of the pontine projection to lateral cerebellar areas in the rat: dual zones in the pons. *Brain Res* 139:340–347
- Catz N, Thier P (2007) Neural control of saccadic eye movements. *Dev Ophthalmol* 40:52–75
- Coffman KA, Dum RP, Strick PL (2011) Cerebellar vermis is a target of projections from the motor areas in the cerebral cortex. *Proc Natl Acad Sci USA* 108:16068–16073. doi:[10.1073/pnas.1107904108](https://doi.org/10.1073/pnas.1107904108)
- D’Mello AM, Stoodley CJ (2015) Cerebro-cerebellar circuits in autism spectrum disorder. *Front Neurosci* 9:408. doi:[10.3389/fnins.2015.00408](https://doi.org/10.3389/fnins.2015.00408)
- Emmers R, Akert K (1963) *A stereotaxic Atlas of the Brain of the Squirrel Monkey (Saimiri sciureus)*. The University of Wisconsin Press, Madison
- Fujita H, Sugihara I (2013) Branching patterns of olivocerebellar axons in relation to the compartmental organization of the cerebellum. *Front Neural Circuits* 7:3. doi:[10.3389/fncir.2013.00003](https://doi.org/10.3389/fncir.2013.00003)
- Fujita H, Oh-Nishi A, Obayashi S, Sugihara I (2010) Organization of the marmoset cerebellum in three-dimensional space: lobulation, aldolase C compartmentalization and axonal projection. *J Comp Neurol* 518:1764–1791. doi:[10.1002/cne.22301](https://doi.org/10.1002/cne.22301)
- Fujita H, Morita N, Furuichi T, Sugihara I (2012) Clustered fine compartmentalization of the mouse embryonic cerebellar cortex and its rearrangement into the postnatal striped configuration. *J Neurosci* 32:15688–15703. doi:[10.1523/JNEUROSCI.1710-12.2012](https://doi.org/10.1523/JNEUROSCI.1710-12.2012)
- Fujita H, Aoki H, Ajioka I, Yamazaki M, Abe M, Oh-Nishi A, Sakimura K, Sugihara I (2014) Detailed expression pattern of aldolase C (Aldoc) in the cerebellum, retina and other areas of the CNS studied in Aldoc-Venus knock-in mice. *PLoS One* 9:e86679. doi:[10.1371/journal.pone.0086679](https://doi.org/10.1371/journal.pone.0086679)
- Glickstein M, May JG 3rd, Mercier BE (1985) Corticopontine projection in the macaque: the distribution of labelled cortical cells after large injections of horseradish peroxidase in the pontine nuclei. *J Comp Neurol* 235:343–359
- Glickstein M, Sultan F, Voogd J (2011) Functional localization in the cerebellum. *Cortex* 47:59–80. doi:[10.1016/j.cortex.2009.09.001](https://doi.org/10.1016/j.cortex.2009.09.001)
- Graybiel AM (1974) Visuo-cerebellar and cerebello-visual connections involving the ventral lateral geniculate nucleus. *Exp Brain Res* 20:303–306
- Groenewegen HJ, Voogd J, Freedman SL (1979) The parasagittal zonation within the olivocerebellar projection. II. Climbing fiber distribution in the intermediate and hemispheric parts of cat cerebellum. *J Comp Neurol* 183:551–601
- Hanson CL, Chen G, Ebner TJ (2000) Role of climbing fibers in determining the spatial patterns of activation in the cerebellar cortex to peripheral stimulation: an optical imaging study. *Neuroscience* 96:317–331
- Hartmann MJ, Bower JM (2001) Tactile responses in the granule cell layer of cerebellar folium crus IIa of freely behaving rats. *J Neurosci* 21:3549–3563
- Hawkes R, Leclerc N (1987) Antigenic map of the rat cerebellar cortex: the distribution of parasagittal bands as revealed by monoclonal anti-Purkinje cell antibody mobQ113. *J Comp Neurol* 256:29–41
- Huerta MF, Krubitzer LA, Kaas JH (1986) Frontal eye field as defined by intracortical microstimulation in squirrel monkeys, owl monkeys, and macaque monkeys: I. Subcortical connections. *J Comp Neurol* 253:415–439
- Ito M, Nisimaru N, Yamamoto M (1977) Specific patterns of neuronal connexions involved in the control of the rabbit’s vestibulo-ocular reflexes by the cerebellar flocculus. *J Physiol* 265:833–854
- Jahn K, Deutschländer A, Stephan T, Kalla R, Wiesmann M, Strupp M, Brandt T (2008) Imaging human supraspinal locomotor centers in brainstem and cerebellum. *Neuroimage* 39:786–792

- Joyner AL, Herrup K, Auerbach BA, Davis CA, Rossant J (1991) Subtle cerebellar phenotype in mice homozygous for a targeted deletion of the *En-2* homeobox. *Science* 251:1239–1243. doi:[10.1126/science.1672471](https://doi.org/10.1126/science.1672471)
- Kelly RM, Strick PL (2003) Cerebellar loops with motor cortex and prefrontal cortex of a nonhuman primate. *J Neurosci* 23:8432–8444
- Kim CH, Oh SH, Lee JH, Chang SO, Kim J, Kim SJ (2012) Lobule-specific membrane excitability of cerebellar Purkinje cells. *J Physiol* 590:273–288. doi:[10.1111/jphysiol.2011.221846](https://doi.org/10.1111/jphysiol.2011.221846)
- Koekkoek SK, v Alphen AM, vd Burg J, Grosveld F, Galjart N, De Zeeuw CI (1997) Gain adaptation and phase dynamics of compensatory eye movements in mice. *Genes Funct* 1:175–190
- Larsell O (1937) The cerebellum. A review and interpretation. *Arch Neurol Psychiatry* 38:580–607
- Larsell O (1952) The morphogenesis and adult pattern of the lobules and fissures of the cerebellum of the white rat. *J Comp Neurol* 97:281–356
- Larsell O (1953) The cerebellum of the cat and the monkey. *J Comp Neurol* 99:135–199
- Larsell O (1970) The comparative anatomy and histology of the cerebellum from monotremes through apes. The University of Minnesota Press, Minneapolis
- Larsell O, Jansen J (1972) The comparative anatomy and histology of the cerebellum, the human cerebellum, cerebellar connections and cerebellar cortex. The University of Minnesota Press, Minneapolis
- Lisberger SG, Fuchs AF (1978) Role of primate flocculus during rapid behavioral modification of vestibuloocular reflex. I. Purkinje cell activity during visually guided horizontal smooth-pursuit eye movements and passive head rotation. *J Neurophysiol* 41:733–763
- Llinás R, Sasaki K (1989) The functional organization of the olivocerebellar system as examined by multiple Purkinje cell recordings. *Eur J Neurosci* 1:587–602
- Lou JS, Bloedel JR (1992) Responses of sagittally aligned Purkinje cells during perturbed locomotion: synchronous activation of climbing fiber inputs. *J Neurophysiol* 68:570–580
- MacKay WA, Murphy JT (1979) Cerebellar modulation of reflex gain. *Prog Neurobiol* 13:361–417
- Madigan JC, Carpenter MB (1971) Cerebellum of the Rhesus Monkey, Atlas of Lobules, Laminae, and Folia, in Sections. University Park Press, Baltimore
- Marani E, Voogd J (1979) The morphology of the mouse cerebellum. *Acta Morphol Neerl Scand* 17:33–52
- Martinez S, Andreu A, Mecklenburg N, Echevarria D (2013) Cellular and molecular basis of cerebellar development. *Front Neuroanat* 7:18. doi:[10.3389/fnana.2013.00018](https://doi.org/10.3389/fnana.2013.00018)
- Marzban H, Hawkes R (2011) On the architecture of the posterior zone of the cerebellum. *Cerebellum* 10:422–434. doi:[10.1007/s12311-010-0208-3](https://doi.org/10.1007/s12311-010-0208-3)
- Mihailoff GA, Burne RA, Azizi SA, Norell G, Woodward DJ (1981) The pontocerebellar system in the rat: an HRP study. II. Hemispherical components. *J Comp Neurol* 197:559–577
- Nieuwenhuys R, Voogd J, Van Huijzen C (2008) The human central nervous system, 4th edn. Springer, Berlin
- Ozden I, Dombeck DA, Hoogland TM, Tank DW, Wang SS (2012) Widespread state-dependent shifts in cerebellar activity in locomoting mice. *PLoS One* 7:e42650. doi:[10.1371/journal.pone.0042650](https://doi.org/10.1371/journal.pone.0042650)
- Ozol K, Hayden JM, Oberdick J, Hawkes R (1999) Transverse zones in the vermis of the mouse cerebellum. *J Comp Neurol* 412:95–111
- Paxinos G, Franklin KBJ (2001) The mouse brain in stereotaxic coordinates, 2nd edn. Academic Press, San Diego
- Paxinos G, Watson C (2007) The rat brain in stereotaxic coordinates, 6th edn. Academic Press, San Diego
- Paxinos G, Huang X-F, Toga AW (2000) The rhesus monkey brain, in stereotaxic coordinates. Academic Press, San Diego
- Paxinos G, Huang XF, Petrides M, Toga AW (2009) The rhesus monkey brain, in stereotaxic coordinates, 2nd edn. Academic-Elsevier, Amsterdam
- Paxinos G, Watson C, Petrides M, Rosa M, Tokuno H (2011) The marmoset brain in stereotaxic coordinates. Academic Press, San Diego
- Pijpers A, Apps R, Pardoe J, Voogd J, Ruigrok TJH (2006) Precise spatial relationships between mossy fibers and climbing fibers in rat cerebellar cortical zones. *J Neurosci* 26:12067–12080
- Quy PN, Fujita H, Sakamoto Y, Na J, Sugihara I (2011) Projection patterns of single mossy fiber axons originating from the dorsal column nuclei mapped on the compartments in the rat cerebellar cortex. *J Comp Neurol* 519:874–899. doi:[10.1002/cne.22555](https://doi.org/10.1002/cne.22555)
- Sarna JR, Marzban H, Watanabe M, Hawkes R (2006) Complementary stripes of phospholipase C $\beta$ 3 and C $\beta$ 4 expression by Purkinje cell subsets in the mouse cerebellum. *J Comp Neurol* 496:303–313
- Sato Y, Kawasaki T (1984) Functional localization in the three floccular zones related to eye movement control in the cat. *Brain Res* 290:25–31
- Schmahmann JD, Pandya DN (1997) Anatomic organization of the basilar pontine projections from prefrontal cortices in rhesus monkey. *J Neurosci* 17:438–458
- Schmahmann JD, Doyon J, McDonald D, Holmes C, Lavoie K, Hurwitz AS, Kabani N, Toga A, Evans A, Petrides M (1999) Three-dimensional MRI atlas of the human cerebellum in proportional stereotaxic space. *Neuroimage* 10:233–260
- Serapide MF, Panto MR, Parenti R, Zappala A, Cicirata F (2001) Multiple zonal projections of the basilar pontine nuclei to the cerebellar cortex of the rat. *J Comp Neurol* 430:471–484
- Sgaier SK, Lao Z, Villanueva MP, Berenshteyn F, Stephen D, Turnbull RK, Joyner AL (2007) Genetic subdivision of the tectum and cerebellum into functionally related regions based on differential sensitivity to engrailed proteins. *Development* 134:2325–2335
- Shambes GM, Gibson JM, Welker W (1978) Fractured somatotopy in granule cell tactile areas of rat cerebellar hemispheres revealed by micromapping. *Brain Behav Evol* 15:94–140
- Shidara M, Kawano K (1993) Role of Purkinje cells in the ventral paraflocculus in short-latency ocular following responses. *Exp Brain Res* 93:185–195
- Shook BL, Schlag-Rey M, Schlag J (1990) The primate supplementary eye field. I. Comparative aspects of mesencephalic and pontine connections. *J Comp Neurol* 301:618–642
- Sillitoe RV, Marzban H, Larouche M, Zahedi S, Affanni J, Hawkes R (2005) Conservation of the architecture of the anterior lobe vermis of the cerebellum across mammalian species. *Prog Brain Res* 148:283–297
- Smaers JB (2014) Modeling the evolution of the cerebellum: from macroevolution to function. *Prog Brain Res* 210:193–216. doi:[10.1016/B978-0-444-63356-9.00008-X](https://doi.org/10.1016/B978-0-444-63356-9.00008-X)
- Smith GE (1902) The primary subdivision of the mammalian cerebellum. *J Anat Physiol* 36:381–385
- Springer MS, Stanhope MJ, Madsen O, de Jong WW (2004) Molecules consolidate the placental mammal tree. *Trends Ecol Evol* 19:430–438
- Steele CJ, Anwander A, Bazini PL, Trampel R, Schaefer A, Turner R, Ramnani N, Villringer A (2016) Human cerebellar sub-millimeter diffusion imaging reveals the motor and non-motor topography of the dentate nucleus. *Cereb Cortex*. doi:[10.1093/cercor/bhw258](https://doi.org/10.1093/cercor/bhw258) (Epub)

- Stoodley CJ, Schmähmann JD (2009) Functional topography in the human cerebellum: a meta-analysis of neuroimaging studies. *Neuroimage* 44:489–501
- Strick PL, Dum RP, Fiez JA (2009) Cerebellum and nonmotor function. *Annu Rev Neurosci* 32:413–434. doi:[10.1146/annurev.neuro.31.060407.125606](https://doi.org/10.1146/annurev.neuro.31.060407.125606)
- Sudarov A, Joyner AL (2007) Cerebellum morphogenesis: the foliation pattern is orchestrated by multi-cellular anchoring centers. *Neural Dev* 2:26
- Sugihara I, Quy PN (2007) Identification of aldolase C compartments in the mouse cerebellar cortex by olivocerebellar labeling. *J Comp Neurol* 500:1076–1092
- Sugihara I, Shinoda Y (2004) Molecular, topographic and functional organization of the cerebellar cortex: a study with combined aldolase C and olivocerebellar labeling. *J Neurosci* 24:8771–8785
- Sugihara I, Shinoda Y (2007) Molecular, topographic and functional organization of the cerebellar nuclei: analysis by three-dimensional mapping of the olivonuclear projection and aldolase C labeling. *J Neurosci* 27:9696–9710
- Sugihara I, Wu HS, Shinoda Y (2001) The entire trajectories of single olivocerebellar axons in the cerebellar cortex and their contribution to cerebellar compartmentalization. *J Neurosci* 21:7715–7723
- Sugihara I, Ebata S, Shinoda Y (2004) Functional compartmentalization in the flocculus and the ventral dentate and dorsal group y nuclei: an analysis of single olivocerebellar axonal morphology. *J Comp Neurol* 470:113–133
- Sugihara I, Fujita H, Na J, Quy PN, Li BY, Ikeda D (2009) Projection of reconstructed single Purkinje cell axons in relation to the cortical and nuclear aldolase C compartments of the rat cerebellum. *J Comp Neurol* 512:282–304. doi:[10.1002/cne.21889](https://doi.org/10.1002/cne.21889)
- Sultan F, Augath M, Hamodeh S, Murayama Y, Oeltermann A, Rauch A, Thier P (2012) Unravelling cerebellar pathways with high temporal precision targeting motor and extensive sensory and parietal networks. *Nat Commun* 3:924. doi:[10.1038/ncomms1912](https://doi.org/10.1038/ncomms1912)
- Suzuki L, Coulon P, Sabel-Goedknecht EH, Ruigrok TJ (2012) Organization of cerebral projections to identified cerebellar zones in the posterior cerebellum of the rat. *J Neurosci* 32:10854–10869. doi:[10.1523/JNEUROSCI.0857-12.2012](https://doi.org/10.1523/JNEUROSCI.0857-12.2012)
- Swanson LW (1998) *Brain maps: structure of the rat brain*, 2nd edn. Elsevier, Amsterdam
- Voogd J (2004) Cerebellum. In: Paxinos G (ed) *The rat nervous system*, 3rd edn. Elsevier Academic Press, Amsterdam, pp 205–242
- Voogd J, Barmack NH (2006) Oculomotor cerebellum. *Prog Brain Res* 151:231–268
- Voogd J, Pardoe J, Ruigrok TJH, Apps R (2003) The distribution of climbing and mossy fiber collateral branches from the copula pyramidis and the paramedian lobule: congruence of climbing fiber cortical zones and the pattern of zebren banding within the rat cerebellum. *J Neurosci* 23:4645–4656
- Wadiche JI, Jahr CE (2005) Patterned expression of Purkinje cell glutamate transporters controls synaptic plasticity. *Nat Neurosci* 8:1329–1334
- Watson TC, Becker N, Apps R, Jones MW (2014) Back to front: cerebellar connections and interactions with the prefrontal cortex. *Front Syst Neurosci* 8:4. doi:[10.3389/fnsys.2014.00004](https://doi.org/10.3389/fnsys.2014.00004)
- Welker W (1987) Spatial organization of somatosensory projections to granule cell cerebellar cortex: functional and connective implications of fractured somatotopy (summary of Wisconsin studies). In: King JS (ed) *New concepts in cerebellar neurobiology*. Liss, New York, pp 239–280
- Welsh JP, Lang EJ, Sugihara I, Llinás R (1995) Dynamic organization of motor control within the olivocerebellar system. *Nature* 374:453–457
- Wu HS, Sugihara I, Shinoda Y (1999) Projection patterns of single mossy fibers originating from the lateral reticular nucleus in the rat cerebellar cortex and nuclei. *J Comp Neurol* 411:97–118